S. Gadgil · S. Sajani

Monsoon precipitation in the AMIP runs

Abstract We present an analysis of the seasonal precipitation associated with the African, Indian and the Australian-Indonesian monsoon and the interannual variation of the Indian monsoon simulated by 30 atmospheric general circulation models undertaken as a special diagnostic subproject of the Atmospheric Model Intercomparison Project (AMIP). The seasonal migration of the major rainbelt observed over the African region, is reasonably well simulated by almost all the models. The Asia West Pacific region is more complex because of the presence of warm oceans equatorward of heated continents. Whereas some models simulate the observed seasonal migration of the primary rainbelt, in several others this rainbelt remains over the equatorial oceans in all seasons. Thus, the models fall into two distinct classes on the basis of the seasonal variation of the major rainbelt over the Asia West Pacific sector, the first (class I) are models with a realistic simulation of the seasonal migration and the major rainbelt over the continent in the boreal summer; and the second (class II) are models with a smaller amplitude of seasonal migration than observed. The mean rainfall pattern over the Indian region for July-August (the peak monsoon months) is even more complex because, in addition to the primary rainbelt over the Indian monsoon zone (the monsoon rainbelt) and the secondary one over the equatorial Indian ocean, another zone with significant rainfall occurs over the foothills of Himalayas just north of the monsoon zone. Eleven models simulate the monsoon rainbelt reasonably realistically. Of these, in the simulations of five belonging to class I, the monsoon rainbelt over India in the summer is a manifestation of the seasonal migration of the planetary scale system. However in those belonging to class II it is associated with a more localised system. In several models, the oceanic rainbelt dominates the continental one. On the whole, the skill in simulation of excess/deficit summer monsoon rainfall over the Indian region is found to be much larger for models of class I than II, particularly for the ENSO associated seasons. Thus, the classification based on seasonal mean patterns is found to be useful for interpreting the simulation of interannual variation. The mean rainfall pattern of models of class I is closer to the observed and has a higher pattern correlation coefficient than that of class II. This supports Sperber and Palmer's (1996) result of the association of better simulation of interannual variability with better simulation of the mean rainfall pattern. The hypothesis, that the skill of simulation of the interannual variation of the all-India monsoon rainfall in association with ENSO depends upon the skill of simulation of the seasonal variation over the Asia West Pacific sector, is supported by a case in which we have two versions of the model where NCEP1 is in class II and NCEP2 is in class I. The simulation of the interannual variation of the local response over the central Pacific as well as the all-India monsoon rainfall are good for NCEP2 and poor for NCEP1. Our results suggest that when the model climatology is reasonably close to observations, to achieve a realistic simulation of the interannual variation of all-India monsoon rainfall associated with ENSO, the focus should be on improvement of the simulation of the seasonal variation over the Asia West Pacific sector rather than further improvement of the simulation of the mean rainfall pattern over the Indian region.

S. Gadil, S. Sajani (✉)
Centre for Atmospheric and Oceanic Sciences,
Indian Institute of Science,
Bangalore - 560 012, India
E-mail: sulo@caos.iisc.ernet.in

1 Introduction

There have been several studies of the Indian monsoon with atmospheric general circulation models (GCMs)

since the pioneering investigations by Manabe et al. (1974) and Hahn and Manabe (1975). The last decade has witnessed rapid developments in GCMs building on detailed investigations of the physical parametrisations (e.g. Slingo 1987; Miller et al. 1992; Sud and Walker 1992) and advances in numerics and computer power which made higher resolution runs possible. It has been found that simulation of the monsoon rainfall over India is sensitive to the physical parametrisations as well as numerics and resolution. Manabe et al. (1979) found a dramatic improvement in monsoon simulation when the GFDL model was recast in spectral form, without any change in physics. Sperber et al. (1994) showed great sensitivity to horizontal resolution. Changes in the NCEP model (Kanamitsu et al. 1990) to include biosphere effects led to great changes in the simulated rainfall pattern (TOGA 1990). Fennessy and Shukla (1994) and Fennessy et al. (1994) found the monsoon rainfall in the model to be sensitive to the manner in which orography was incorporated. Slingo et al. (1992, 1994) demonstrated the impact of the nature of convective parametrisation and Laval et al. (1996) of the nature of hydrological parametrisation.

There is considerable evidence of a link between the variability of the Indian monsoon and El Niño Southern Oscillation (ENSO) (Sikka 1980; Rasmusson and Carpenter 1983; Ropelewski and Halpert 1987, 1996 etc.). The success in simulating and predicting ENSO during the Tropical Ocean and Global Atmosphere (TOGA) led to renewed interest in the simulation of the monsoon and its variability on seasonal to interannual scale. Systematic intercomparison of the simulation of the two seasons of 1987 and 1988, in which the ENSO phase as well as the intensity of the Indian monsoon were strongly contrasting, were carried out by the TOGA Monsoon Numerical Experimentation Group. In one such study, Palmer et al. (1992) showed that a large fraction of the variability of the simulated Indian monsoon was forced by the sea surface temperature (SST) variations over the Pacific.

The Atmospheric Intercomparison Project (AMIP, Gates 1992) provided a unique opportunity for systematic studies of the response of many atmospheric GCMs to observed variations in SST during the decade of 1979–1988. This period is particularly interesting because of the occurrence of two major events of ENSO 1982–1983, 1987–1988 which were associated with large fluctuations of the Indian monsoon. An understanding of how well the models can simulate the monsoon variations, when forced by the observed variation of SST, is important for assessing the potential for generating predictions of the Indian monsoon on seasonal to interannual scale.

We present here an analysis of the AMIP runs of 30 models carried out under the AMIP diagnostic subproject on the simulation of the monsoon rainfall and its variation. Although the focus is on the Indian monsoon, we first consider briefly the simulation of the seasonal variation of the major tropical rainbelts over the monsoonal regions of the world (Sect. 3). The simulation of the mean rainfall pattern during the peak monsoon months of July and August over the Indian region is discussed in Sect. 4 and the interannual variation of the Indian summer monsoon during the AMIP decade and its teleconnection with the Pacific in Sect. 5.

2 Models and data

In AMIP, all the major atmospheric GCMs have been run for the period January 1979–December 1988 with lower boundary conditions of SST and sea ice specified from observations (Gates 1992). The outputs of runs of a large number of models have been made available in standard format, after quality control checks by the Program for Climate Model Diagnosis and Intercomparison (PCMDI) at the Lawrence Livermore National Laboratory. The PCMDI has also supplied data on the observed SST. The details of the runs of the 30 models analysed here (Table 1) are available in the AMIP documentation by Phillips (1994). Dr. S. Saha of the National Center for Environmental Prediction (NCEP, USA) generated the results for an AMIP run with a revised version of the NCEP model and sent these to us for analysis. The new version of the NCEP model (henceforth referred to as NCEP2) differs from the old version (henceforth NCEP1) in physics as well as resolution. The resolution is changed from T40L18 to T62L28. In NCEP1 convection is parametrised following Kuo (1965), Sela (1980) and Tiedtke (1983) whereas the parametrisation in the NCEP2 model follows Pan and Wu (1995) which is based on Arakawa and Shubert (1974), simplified by Grell (1993) and Tiedtke (1983). In NCEP1, the surface fluxes of momentum, heat and moisture are stability dependent, while a new PBL parametrisation scheme (Hong and Pan 1996) has been implemented in NCEP2. Land surface processes are based on Miyakoda and Sirutis (1986) in NCEP1 and on Pan and Mahrt (1987) in the NCEP2. The AMIP simulation of the NCEP2 model has also been analyzed along with those of the thirty models supplied by PCMDI.

Several data sets for precipitation and convection have been used for comparison with model simulated precipitation. For precipitation, the data of Legates-Willmott (LW, Legates and Willmott 1990), and a merged data set supplied by NCEP (Schemm et al. 1992; Kalnay et al. 1996; henceforth referred to as NCEP merged data) comprising station data over land and precipitation over the oceans estimated from MSU (Microwave Sounding Unit, Spencer 1993) have been used. In addition, over the Indian region, we have analysed the rainfall data at 366 meteorological observatories, supplied by the India Meteorological Department (IMD), which is henceforth referred to as IMD data, and the all-India rainfall time series derived by Parthasarathy et al. (1994) from IMD data. We have also analysed the frequency of highly reflective clouds (HRC, Garcia 1985) and the outgoing longwave radiation (OLR, Gruber and Krueger 1984).

3 Global perspective

The word 'monsoon' comes from the Arabic word 'mausam' for season and the distinguishing attribute of the monsoonal regions of the world is the seasonal variation in circulation and rainfall (Ramage 1971). Large seasonal variation of the major zones of deep

Table 1 AMIP modeling groups, locations and resolutions

Acronym	AMIP group	Resolution
BMRC	Bureau of Meteorology Research Centre, Australia	R31 L9
CCC	Canadian Centre for Climate Research, Canada	T32 L10
CNRM	Centre National de Recherches Mètèorologiques, France	T42 L30
COLA	Centre for Ocean-Land-Atmosphere Studies, USA	R40 L18
CSIRO	Commonwealth Scientific and Industrial Research Organization, Australia	R21 L9
CSU	Colorado State University, USA	$4^\circ \times 5^\circ$ L17
DERF	Dynamical Extended Range Forecasting, USA	T42 L18
DNM	Department of Numerical Mathematics, Russia	$4^\circ \times 5^\circ$ L7
ECMWF	European Centre for Medium-Range Weather Forecasts, UK	T42 L19
GFDL	Geophysical Fluid Dynamics Laboratory, USA	R30 L14
GISS	Goddard Institute for Space Studies, USA	$4^\circ \times 5^\circ$ L9
GLA	Goddard Laboratory for Atmospheres, USA	$4^\circ \times 5^\circ$ L17
GSFC	Goddard Space Flight Center, USA	$4^\circ \times 5^\circ$ L20
IAP	Institute of Atmospheric Physics, China	$4^\circ \times 5^\circ$ L2
JMA	Japan Meteorological Agency, Japan	T42 L21
LMD	Laboratory de Mètèorologie Dynamique, France	50sin(lat) × 64lon L11
MGO	Main Geophysical Observatory, Russia	T30 L14
MPI	Max-Planck Institut fuer Meteorologie, Germany	T42 L19
MRI	Meteorological Research Institute, Japan	$4^\circ \times 5^\circ$ L15
NCAR	National Center for Atmospheric Research, USA	T42 L18
NCEP1	National Center for Environmental Prediction, USA	T40 L18
NCEP2	National Center for Environmental Prediction, USA	T62 L28
NRL	Naval Research Laboratory, USA	T47 L18
RPN	Recherche en Prèvision Numèrique, Canada	T63 L23
SUNYA	State University of New York at Albany, USA	R15 L12
SNG	State University of New York at Albany/ National Center for Atmospheric Research, USA	T31 L18
UCLA	University of California at Los Angeles, USA	$4^\circ \times 5^\circ$ L15
UGAMP	The UK Universities' Global Atmospheric Modeling Programme, UK	T42 L19
UIUC	University of Illinois at Urbana-Champaign, USA	$4^\circ \times 5^\circ$ L7
UKMO	United Kingdom Meteorological Office, UK	$2.5^\circ \times 3.75^\circ$ L19
YONU	Yonsei University, Korea	$4^\circ \times 5^\circ$ L15

convection and precipitation occurs over the Asia Pacific sector in association with the Asian/Australian monsoon and over the African longitudes in association with the African monsoon (Fig. 1). It is seen that this zone of precipitation/convection over most of the tropics occurs around 10 °S in the austral summer and 10 °N in the boreal summer; the exception is the Asia West Pacific sector where it is displaced farther northward in the boreal summer. The models also exhibit a tendency for the rainbelt to occur around 10° in the summer hemisphere. We first consider the simulation of the mean seasonal rainfall patterns over the monsoonal regions in the AMIP runs. For each region, we compare the simulated seasonal mean precipitation pattern, particularly the latitudinal range and longitudinal extent of the region with significant precipitation, with observations. Henceforth we refer to the region with significant precipitation as 'precipzone'.

3.1 African monsoon

The large seasonal variation over the African region is clearly seen from the observed mean patterns of rainfall during boreal and austral summers (Figs. 1, 2). During the boreal summer, the precipzone extends from the east Atlantic up to about 30 °E, with maximum rainfall occurring a little to the south of 10 °N. This rainfall pattern simulated by a few representative models is shown in Fig. 2. Almost all the models simulate the pattern reasonably well. The exception is the simulation of DNM in which the precipzone is northward of the observed, west of about 10 °E. While the maximum rainfall for a majority of the models is near the observed value, in some models such as the UIUC, the rainbelt is extremely weak whereas in some, such as UGAMP, it is too strong. Several models (such as GFDL, COLA) simulate the high rainfall near the eastern end (which is observed in the LW rainfall) while in others (such as CNRM, SUNYA) the rainfall is more uniform in the east-west direction. If the latitudinal extent of the rainbelt is defined by the latitudes at which 50% of the value of peak is attained, it is about 15° for the observed patterns of precipitation and convection. The latitudinal extent of the simulated rainbelt varies from 10° to 20°, with the largest extent in the simulations of SUNYA, YONU and CSU in which considerable rainfall occurs up to 10 °S.

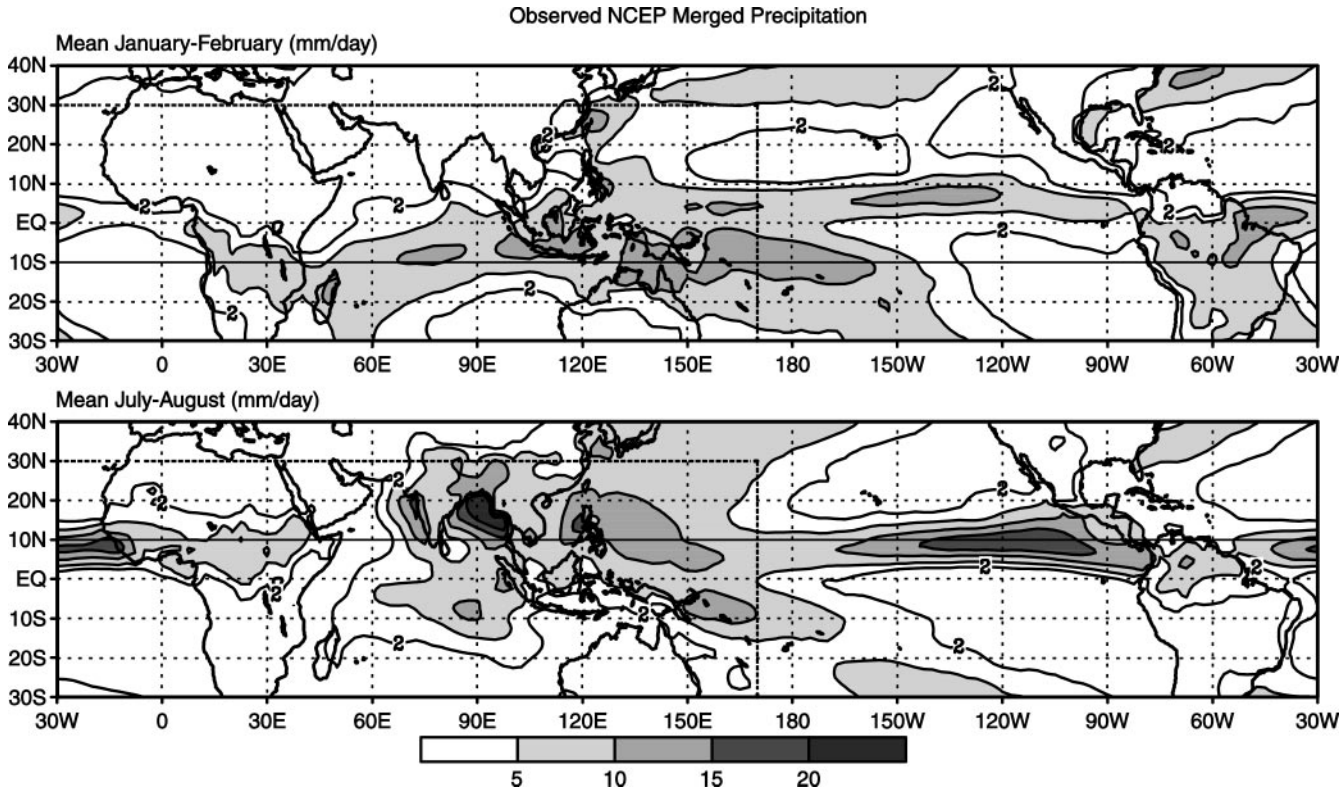

Fig. 1 Observed mean (for the AMIP period) precipitation for January–February (top) and for July–August (bottom). The *box* indicates monsoonal regions of the world as defined by Ramage (1971)

In the austral summer, the precipzone occurs over the southern part of the continent extending from the equator up to about 20 °S with a maximum around 10 °S (Fig. 2). In some models there appear to be small-scale structures with intense rainfall near the east coast, but in a majority of models the rainfall is relatively uniform in the zonal direction. By and large, the location, latitudinal extent as well as the maximum rainfall in this season are well simulated by the models (Fig. 2). Thus, the seasonal migration of the major precipzone over the African longitudes is simulated by all the models and the mean rainfall patterns for the boreal and austral summers are also generally well simulated.

3.2 Australian–Indonesian monsoon

We have analysed the simulation of the seasonal average rainfall associated with two major components of the Asian monsoon, i.e. the Australian–Indonesian monsoon in austral summer and the Indian monsoon in the boreal summer. In this section, we consider briefly the simulation of the mean seasonal rainfall pattern associated with the Australian–Indonesian monsoon and discuss the simulation of the precipitation in the Asia-Pacific sector and of the Indian monsoon in Sections 3.3 and 4.

Indonesia and northern parts of Australia receive a substantial fraction of the annual rainfall during the austral summer (Ramage 1971; McBride 1987). The distribution of the observed rainfall for January–February is shown in Fig. 3. It is seen that the major rainbelt tilts southeastward from the Indonesian region (with the axis between 0 and 5 °S between 110 °E and 120 °E) towards Australia (with the axis around 10 °S between 130 °E and 145 °E). Legates-Willmott precipitation and HRC datasets also exhibit similar pattern over this region.

The rainfall patterns simulated by a few representative models are also shown in Fig. 3. It is seen that the pattern in some of the models (e.g. NCEP2, BMRC, MRI) is fairly realistic. It is interesting that in several models (such as LMD and COLA), the primary rainbelt remains over the equatorial region and a secondary precipitation zone is seen over the Australian region. However, in COLA model simulation, the precipitation pattern over the Australian-Indonesian region is rather realistic. In some models, the Australian monsoon appears to be well simulated but relatively little rainfall occurs over Indonesia (e.g. MGO). In

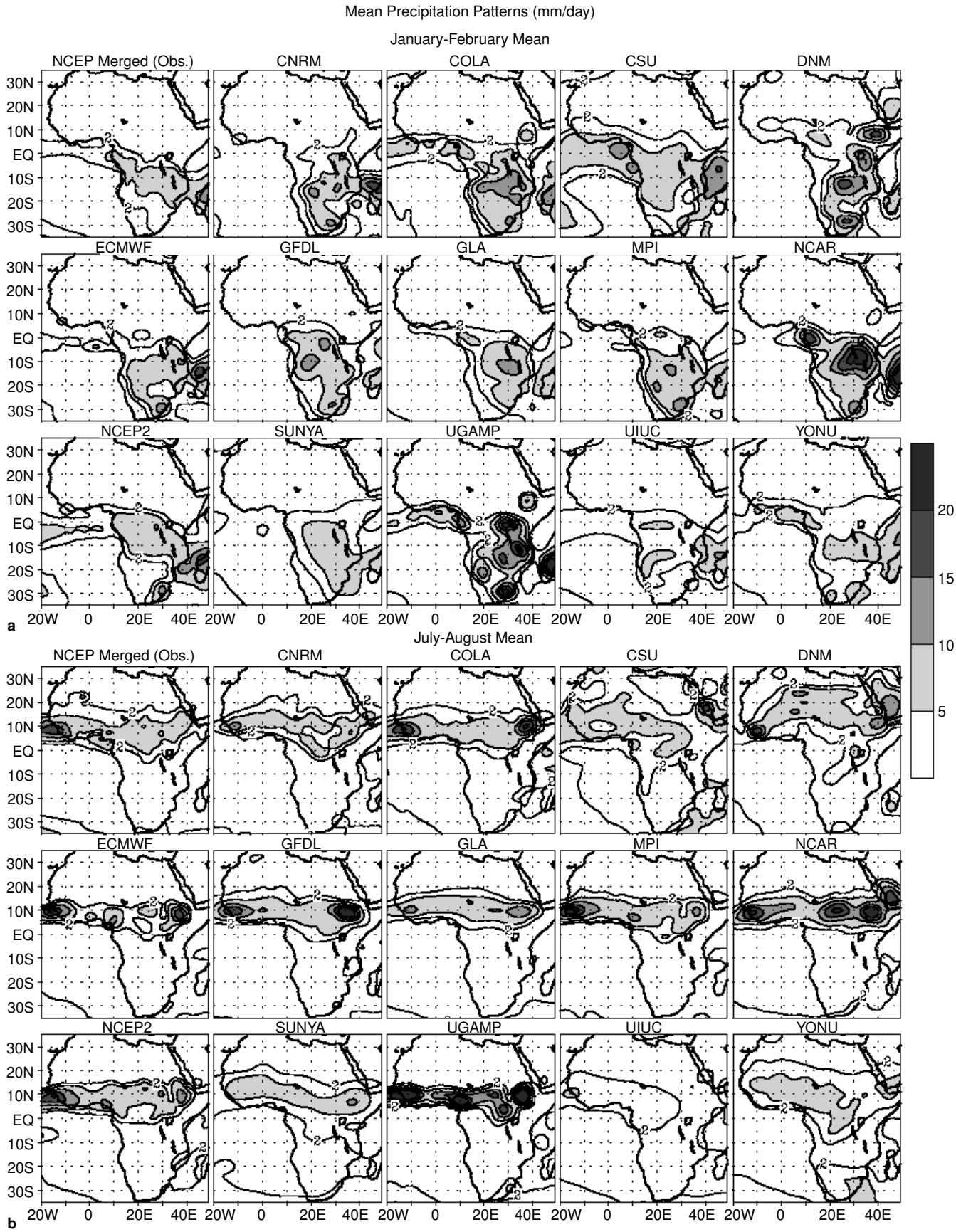

Fig. 2a, b Observed and simulated mean precipitation over the African region for **a** January–February and **b** July–August

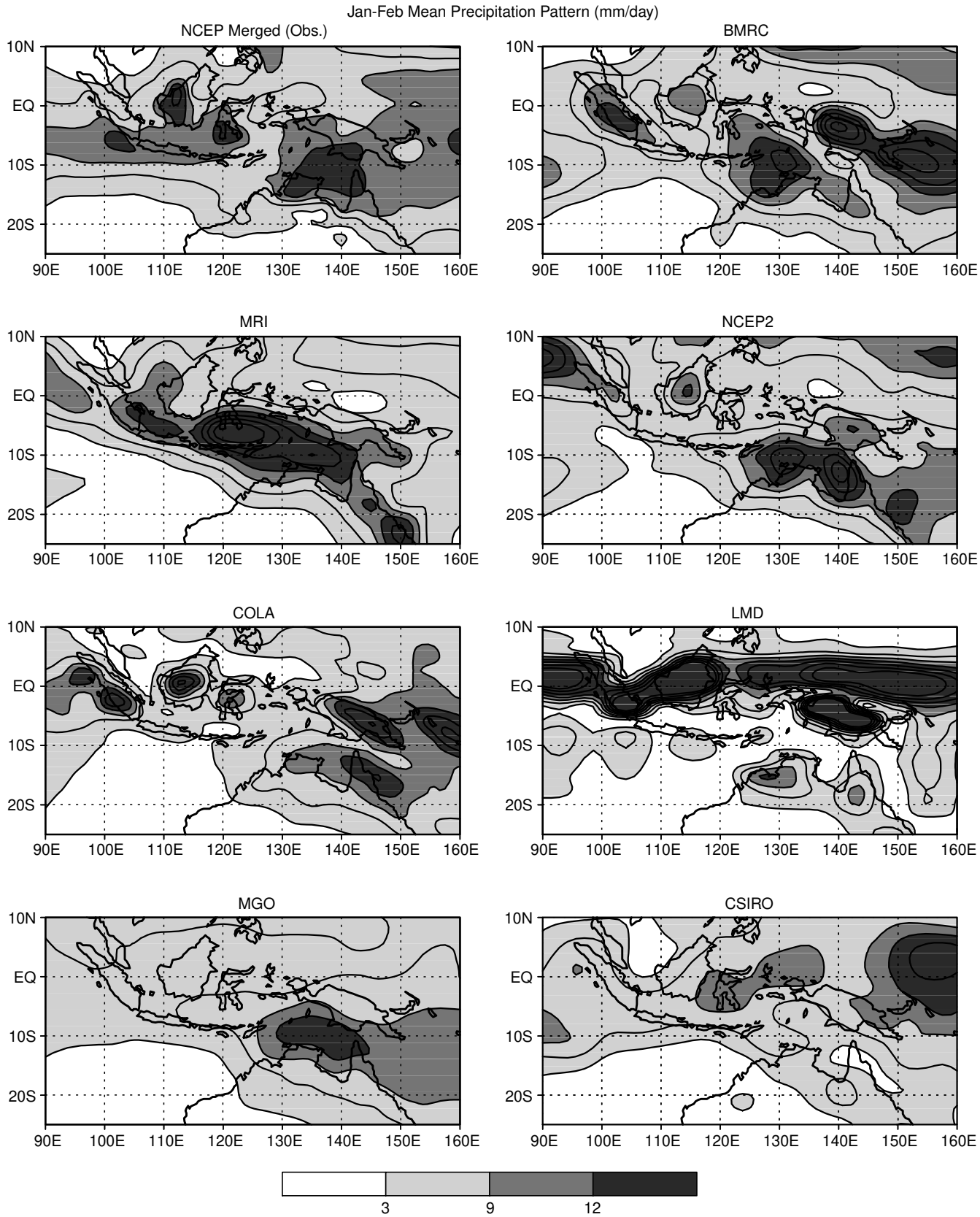

Fig. 3 Observed and simulated mean precipitation for January–February over the Australian-Indonesian region

many models the rainbelt remains zonal throughout the region and equatorward of the observed location north of Australia (e.g. CSIRO). Overall, the simulation of the mean rainfall pattern over this region is not as good as over the African region although a reasonable degree of skill is evident in a number of models.

3.3 Asia–Pacific

In this region, the precipzone (here taken as the region with rainfall greater than 6 mm/day) occurs as a coherent zone over a wide longitudinal range, stretching from the Asian longitudes across the West Pacific in the boreal and austral summers (Fig. 4). The wide longitudinal extent of the system in the boreal summer is also clear from the mean July pattern of the distribution of the heat sources over the region derived by Chen and Li (1981) (from Tao and Chen 1987). The rainbelt with maximum precipitation occurs in the equatorial and near-equatorial regions of the Southern Hemisphere in the austral summer; in the equatorial region in spring and autumn and attains its northernmost position over the western sector (70 °E–120 °E) in the boreal summer with a slight southeastward tilt over the West Pacific (Fig. 4).

The seasonal variation of the latitude of the major rainbelt is also clearly seen in the variation of the mean monthly precipitation for the Asia West Pacific sector (70 °E–140 °E) and the African region (10 °W–40 °E) depicted in Fig. 5. Note that whereas over the African region the latitudinal extent of the precipzone is about 15° throughout the year while the location shifts with season; the latitudinal extent of the precipzone over the Asia West Pacific sector becomes very large in the boreal summer, extending from south of the equator to north of 25 °N. Thus over the Asia Pacific sector, the equatorial region receives rainfall throughout the year, even in the boreal summer when the major rainbelt is located around 15 °N. It is seen from Fig. 4 that within the Asia West Pacific sector, the latitudinal extent is largest around 90 °E. On a daily scale, the latitudinal extent of the tropical convergence zone over this region is somewhat larger than that over Africa but never exceeds 10° (Sikka and Gadgil 1980). The large latitudinal extent of the precipzone on monthly/seasonal scales over the Indian longitudes arises from (1) the existence of a secondary precipzone over the equatorial ocean, with frequent genesis of a tropical convergence zones (TCZ) throughout the summer, and (2) fluctuations of the rainbelt, between this secondary zone and the primary one, over the heated subcontinent on the intraseasonal scale (Sikka and Gadgil 1980; Gadgil 1988). Such meridional fluctuations are also found to occur over the West Pacific (Srinivasan and Smith 1996). Thus, the zone with relatively little meridional variation of the mean precipitation equatorward of 15 °N of the Asia West Pacific sector on the monthly/seasonal scales arises from the intraseasonal fluctuations of the rainbelt over this region.

We consider the seasonal migration of the primary rainbelt over the Asia West Pacific region onto the heated continent in the boreal summer (Figs. 4, 5) to be the most important feature of the seasonal variation over this region. Hence, in assessing the simulations, we give maximum weight to a realistic simulation of the primary rainbelt across the Asia West Pacific region. Relatively, the simulation of the latitudinal extent of the precipzone and a realistic meridional profile (which are likely to depend upon the simulation of the secondary zone over equatorial ocean and, perhaps, intraseasonal fluctuations), will be considered less important.

We find that while some models simulate the seasonal migration and the primary rainbelt during the boreal summer realistically (e.g. GLA model in Fig. 6), in some others the primary rainbelt persists over the equatorial oceans in all the seasons (e.g. UGAMP model in Fig. 6). This suggests a classification of the models on the basis of whether they simulate the seasonal variation in the latitude of the primary rainbelt and its location during the boreal summer realistically (class I) or not (class II). Such a classification of the models is given in Table 2. For some representative class I models, the mean precipitation patterns for the four seasons and the monthly variation of the mean precipitation of the Asia West Pacific sector (70 °E–140 °E) are shown in Fig. 7a. It is seen that, in the simulation of some models of class I, there is not much precipitation over the equatorial oceans in the boreal summer (e.g. GFDL), whereas in some others, there is a distinct secondary precipzone appearing over that region (e.g. NCEP2).

The amplitude of the seasonal migration of the primary rainbelt is much smaller than observed in models of class II (Fig. 7b). For example, in the NCAR simulation, the major rainbelt migrates from a realistic location in the austral summer around 10 °S to around 10 °N in the boreal summer which is equatorward of the observed location. Figure 7b also shows that in models such as MGO, DNM, there is hardly any seasonal migration of the rainbelt over the Pacific, while for DERF there is no seasonal migration over the Indian longitudes. In some models, such as LMD, there is hardly any variation in the major rainbelt with season.

We note that in some models of class II, in the boreal summer, a secondary precipzone is simulated over part of the latitudinal belt where the primary rainbelt is observed. For example, in the July–August simulations of the COLA and ECMWF models (Fig. 7b), in addition to the major rainbelt over the equatorial ocean, a precipzone is simulated between 20 °N and 30 °N centred around 90 °E. However, the longitudinal extent of this zone is much smaller than that of the observed

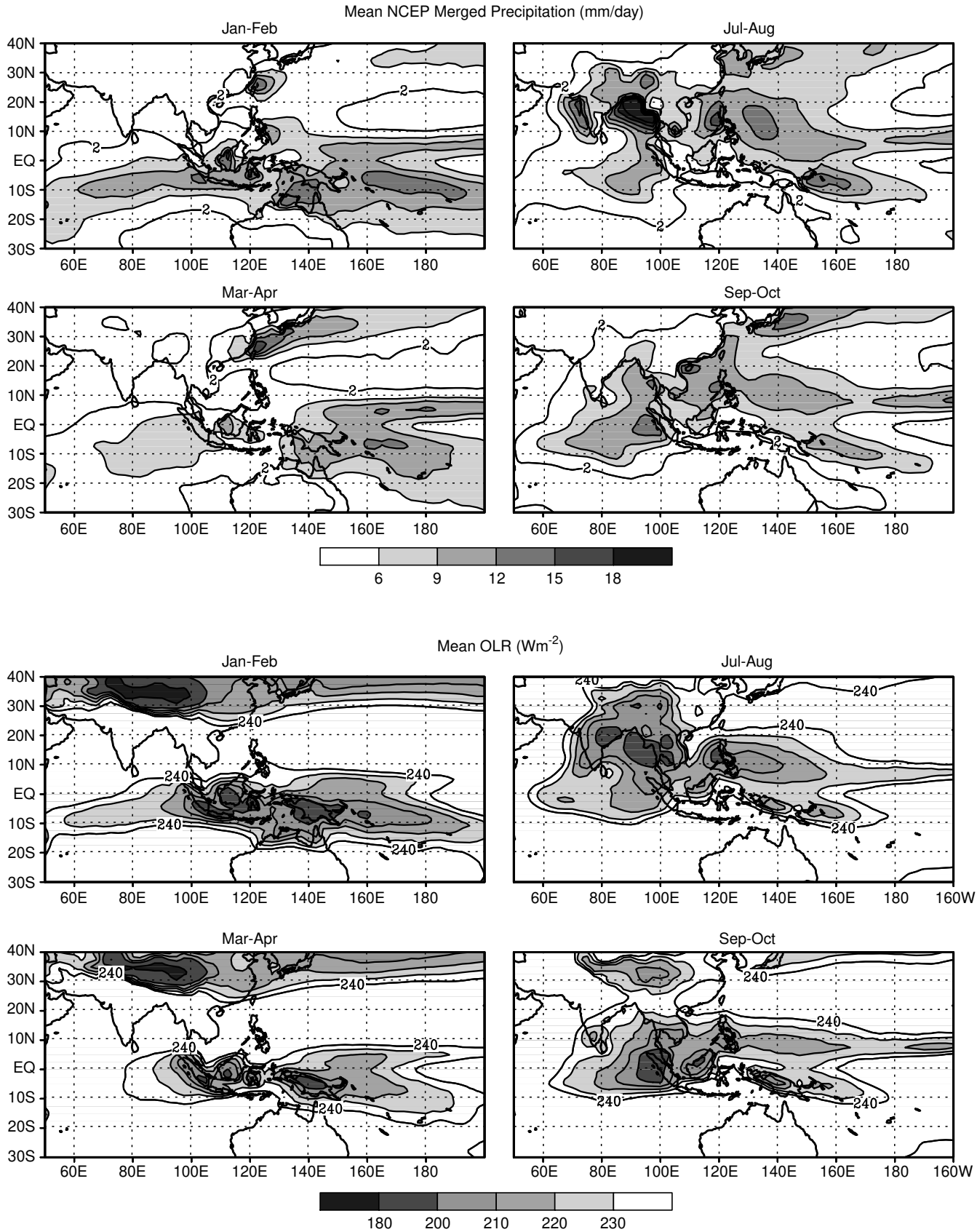

Fig. 4 Seasonal variation of the observed mean precipitation (*upper*) and OLR (*lower*) over the Asia-Pacific region

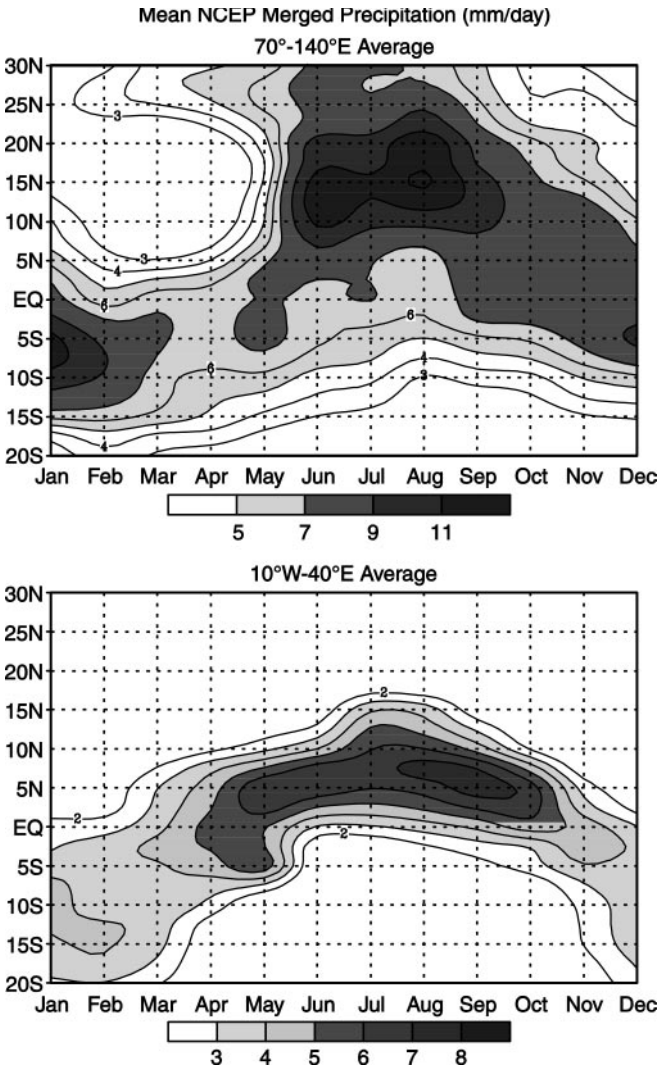

Fig. 5 Variation of the observed monthly mean precipitation over (*top*) the Asia-Pacific (70°–140 °E) region and (*bottom*) the African (10 °W–40 °E) region

rainbelt in this latitudinal range and also smaller than that of the simulated rainbelt in the equatorial regions. Thus, there appears to be a tendency in some models of this class to generate localised/secondary precipitation region over heated continents (Indian or Australian) rather than a seasonal migration of the primary rainbelt. We return to this point in next section.

4 Indian summer monsoon

4.1 Mean rainfall pattern

Most of the rainfall over the Indian subcontinent occurs during the summer monsoon i.e. June–September (Rao 1976). The observed mean patterns of rainfall for the peak monsoon months of July–August over the Indian region are shown in Fig. 8. We compare the mean simulated and observed patterns for July–August, rather than for the entire summer monsoon, because in many models the duration of the rainy season is underestimated. The large-scale monsoon rainfall in the summer is associated with the rainbelt I extending from the head of the Bay of Bengal, west-northwestward across the Indo-Gangetic plain. During the summer monsoon, the monsoon trough and this rainbelt fluctuate within the monsoon zone, north of about 15 °N (Sikka and Gadgil 1980, and references therein). The variation of the location and intensity of the monsoon trough and rainbelt I give rise to the variations in the large-scale monsoon rainfall. The coefficient of variation of the seasonal rainfall is maximum (over 50%) near the western end and minimum (about 20–30%) in the high rainfall zone at the eastern end near the head of the Bay of Bengal (Rao 1976). On the interannual scale, the variation of the all-India monsoon rainfall arises primarily from the variation over western part of the monsoon zone i.e. west of 80 °E (Parthasarathy 1984). Thus, for a model to be useful in predicting variations on the seasonal to interannual scale, it is important that it can simulate rainbelt I and its variability (particularly in the western part) reasonably well. Henceforth we refer to this rainbelt I as the monsoon rainbelt.

Besides the tropical convergence zone over the heated subcontinent with which the primary rainbelt is associated, a TCZ also occurs over the warm waters of the equatorial Indian ocean intermittently throughout the summer (Sikka and Gadgil 1980). This is manifested as a secondary zone of precipitation in the seasonal rainfall patterns (rainbelt II in Fig. 8). Over the Indian region, heavy rainfall also occurs in association with

Table 2 Classes based on the seasonal variation of the precipzone over the Asia West Pacific region

Class I	Class II
BMRC	COLA
CCC	CSU
CNRM	DERF
CSIRO	DNM
GFDL	ECMWF
GISS	IAP
GLA	JMA
GSFC	LMD
MPI	MGO
MRI	NCAR
NCEP2	NCEP1
RPN	NRL
UKMO	SNG
	SUNYA
	UCLA
	UGAMP
	UIUC
	YONU

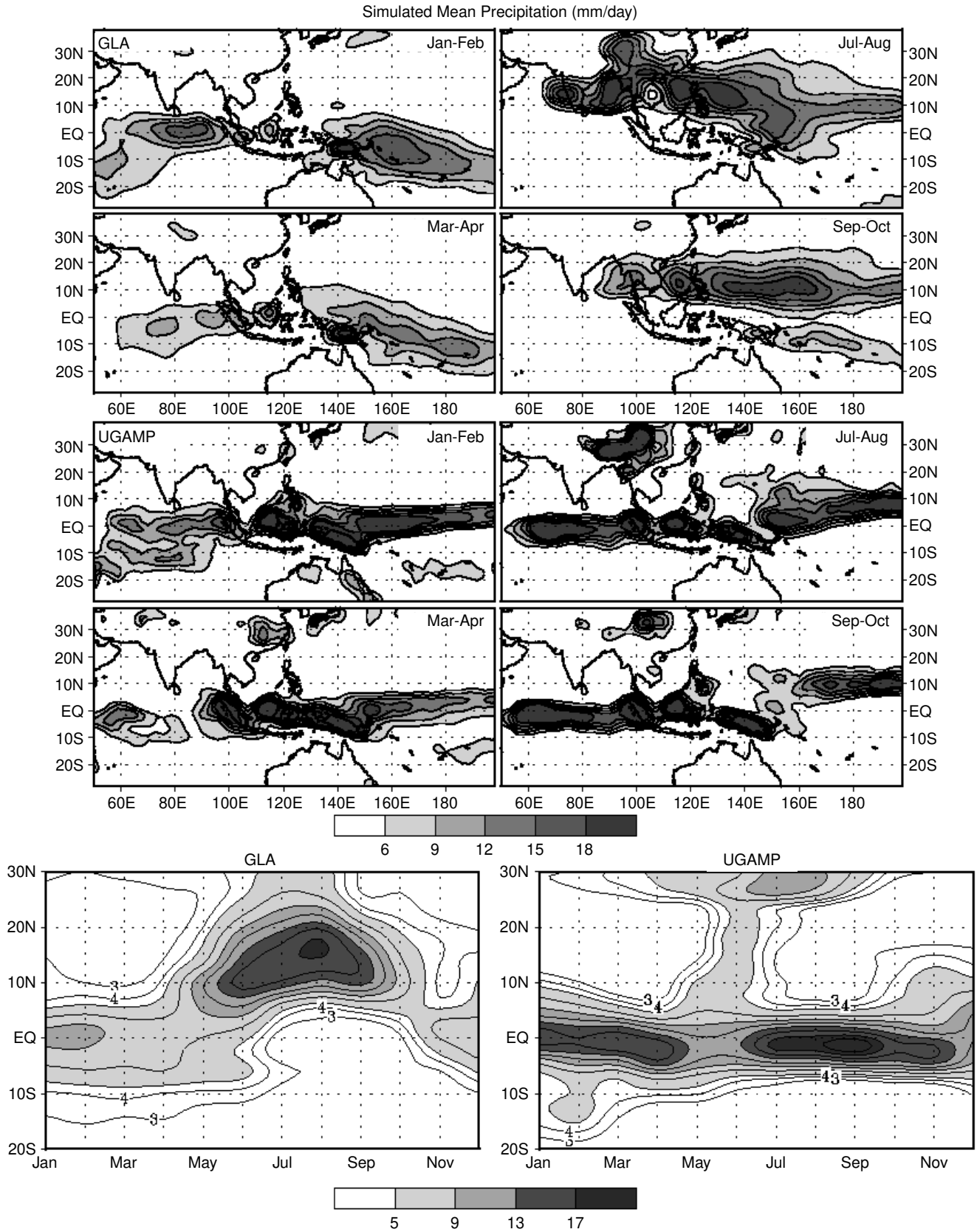

Fig. 6 Simulated mean precipitation for January–February, March–April, July–August and September–October by GLA model (*top*) and UGAMP model (*centre*); variation of the simulated monthly mean precipitation for 70 °E–140 °E sector by GLA and UGAMP models (*bottom*)

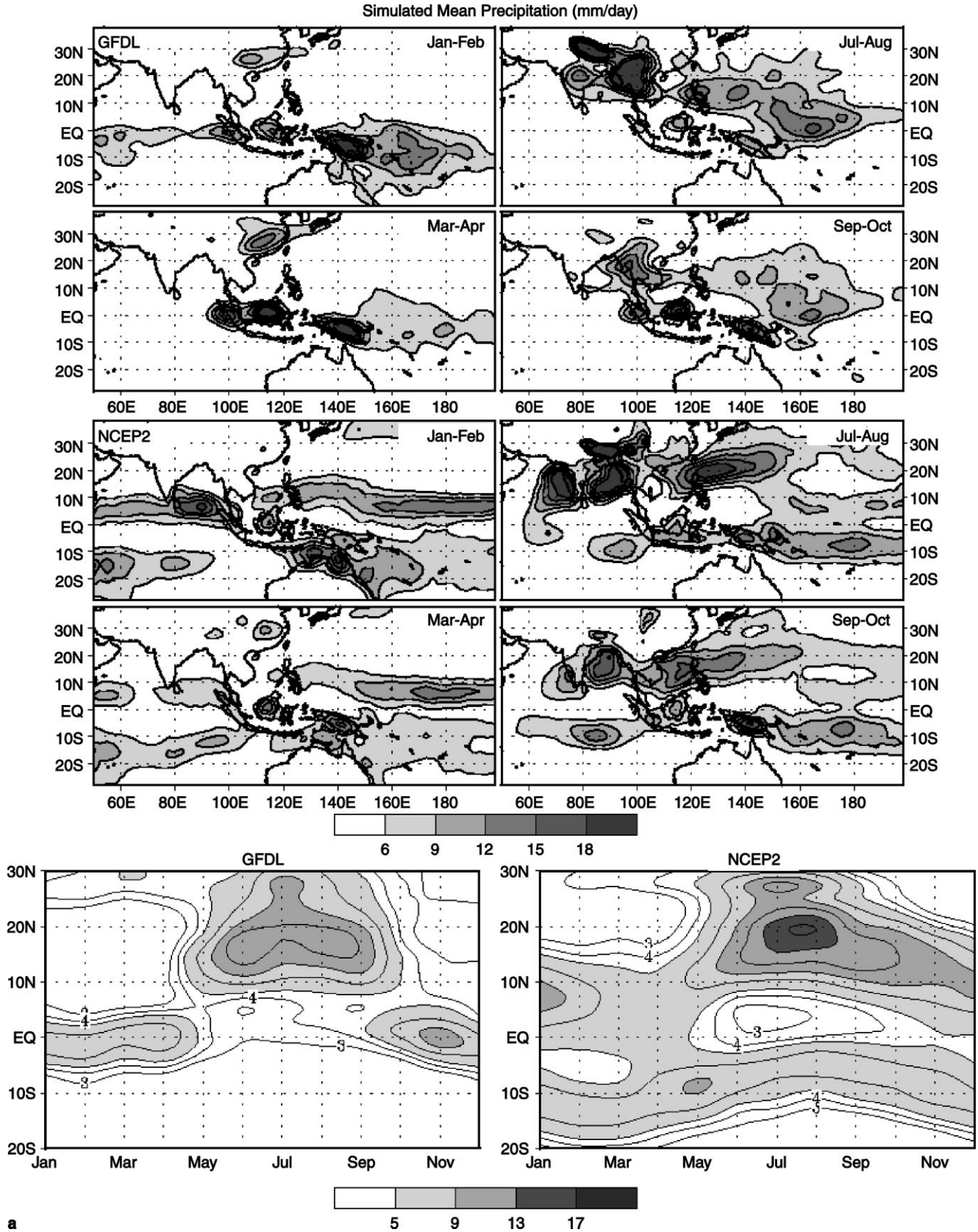

Fig. 7a As in Fig. 6 for models of class I; **b** as in Fig. 6 for models of class II

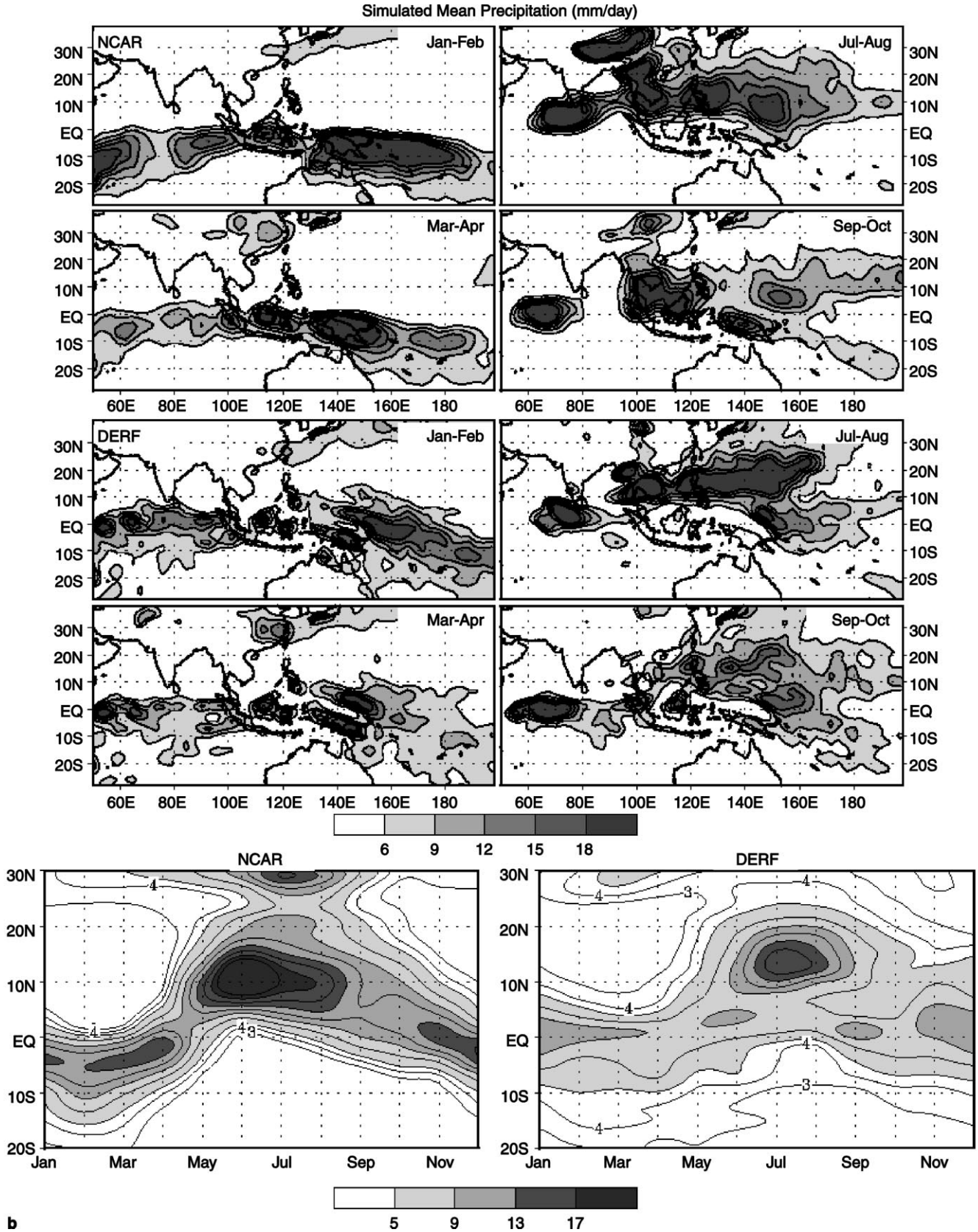

Fig. 7 (*Continued*)

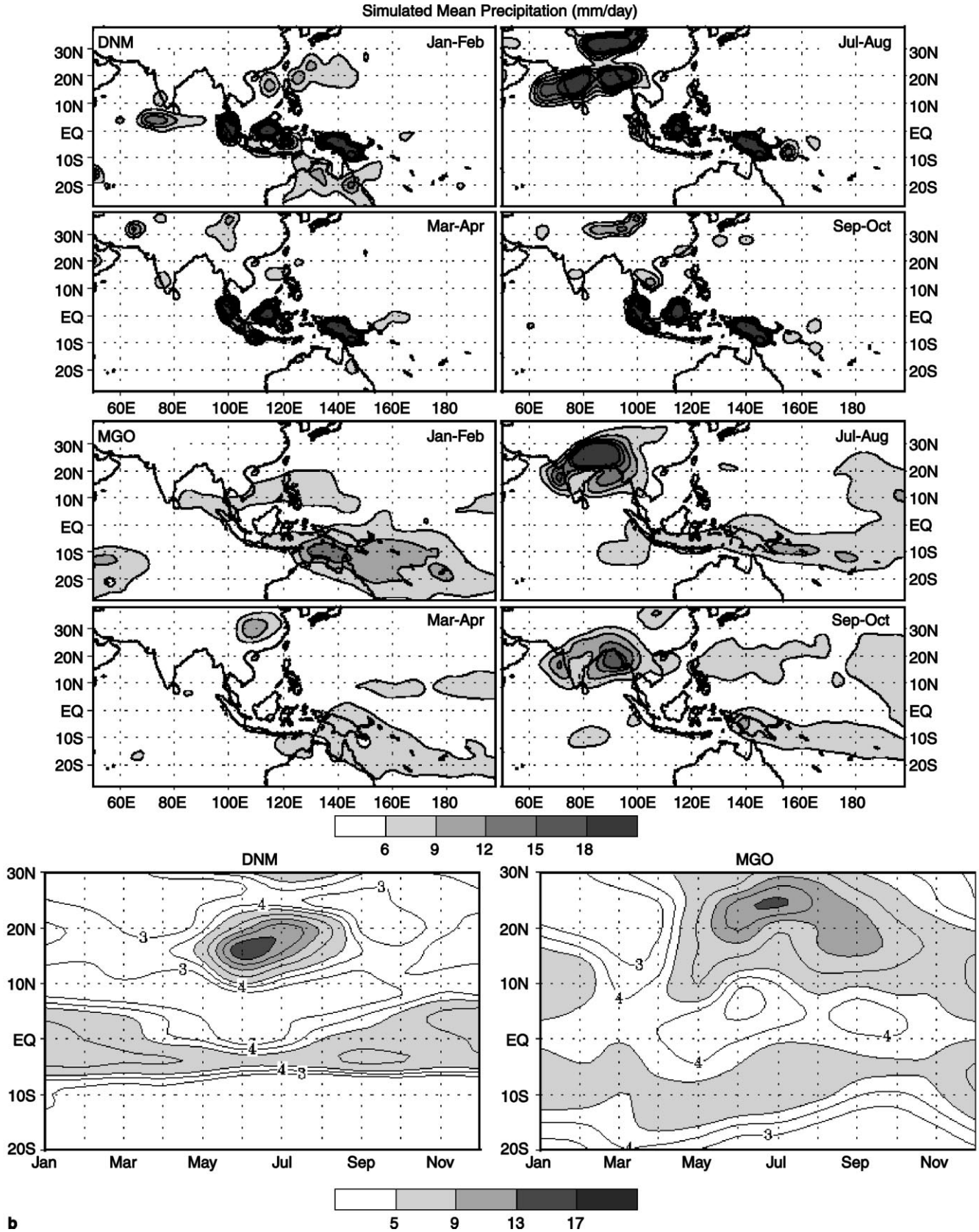

Fig. 7 (*Continued*)

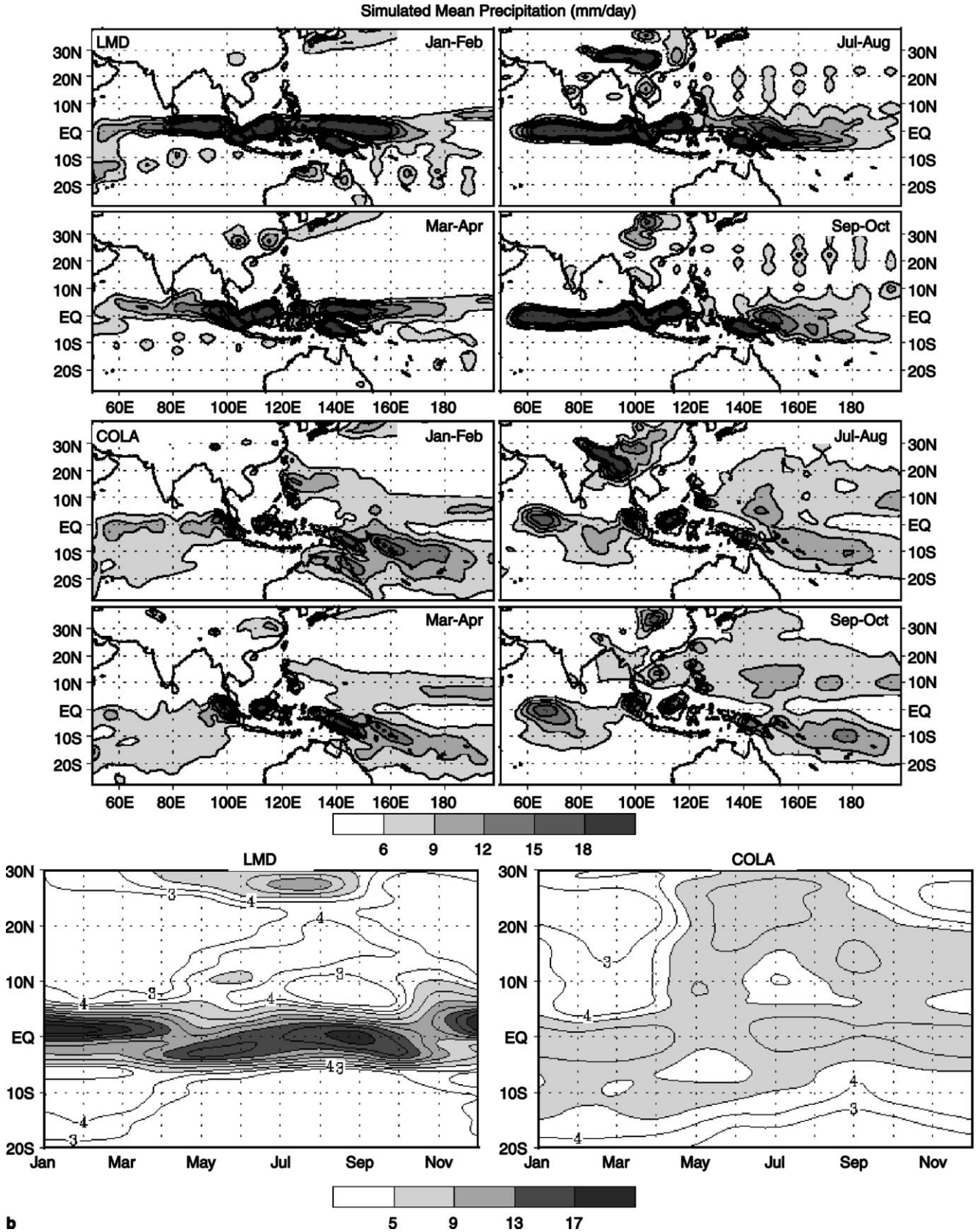

Fig. 7 (*Continued*)

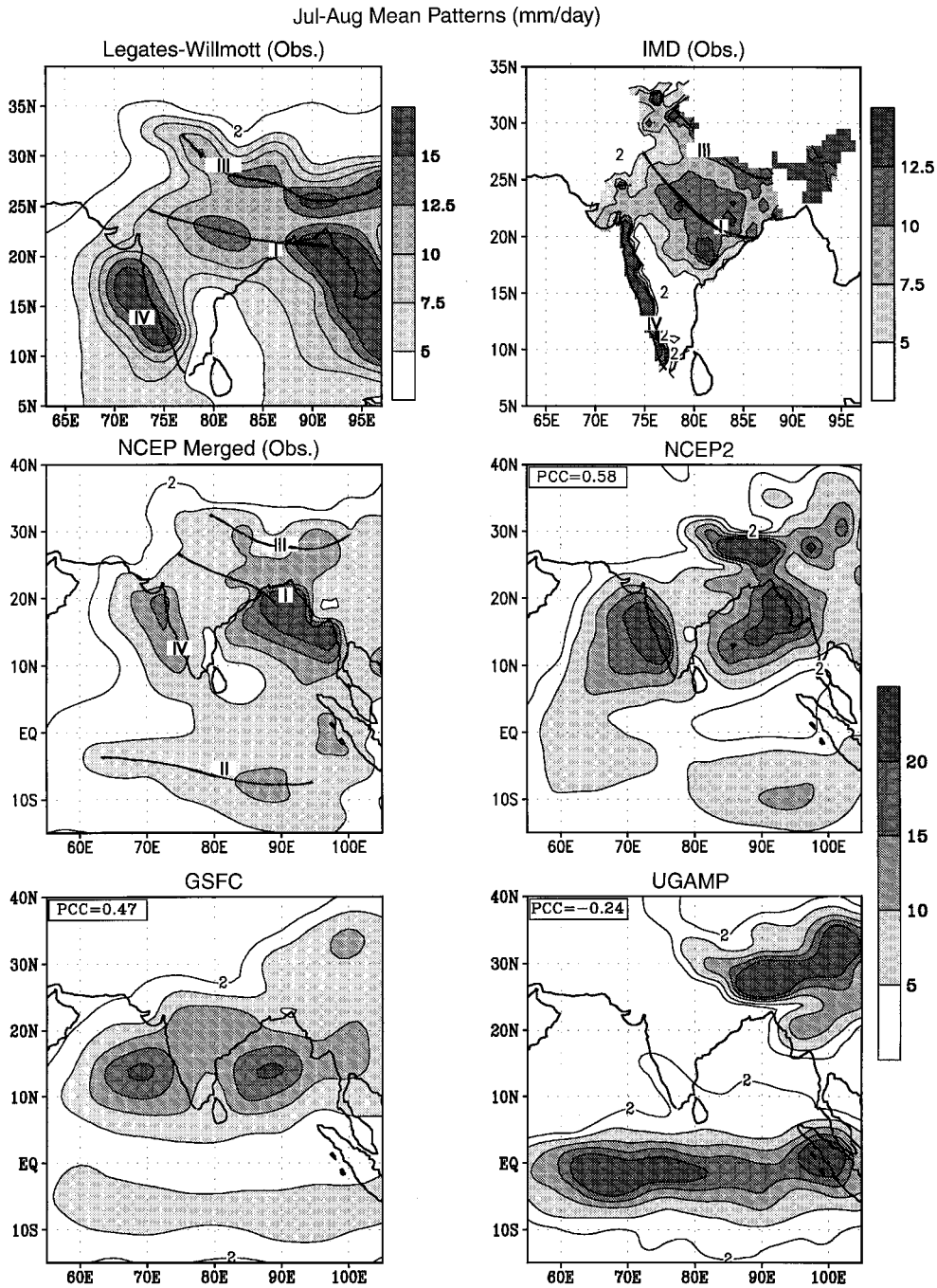

Fig. 8 Observed mean July-August precipitation over the Indian region and typical patterns of simulation of the mean July-August precipitation over the Indian region

the orography of the Himalayas to the north (rainbelt III in Fig. 8) and the western Ghats along the west coast of the peninsula (rainbelt IV in Fig. 8).

The rainfall pattern over the Indian longitudes is extremely complex and not surprisingly, the simulation of the mean summer rainfall pattern over the Indian region has proved to be a difficult task. The simulations of models differ in how realistically the monsoon rainbelt is simulated and in the relative intensities of the other rainbelts. Typical rainfall patterns in models are also illustrated in Fig. 8. The pattern correlation coefficient of the simulated mean July–August rainfall pattern over 70 °E–90 °E; 0–30 °N with the observed NCEP merged data for a common grid of 2.5° is indicated in the top corner. In some, the rainfall over the monsoon zone is realistically simulated (e.g. NCEP2 in Fig. 8). In others, the primary rainbelt is somewhat southward of the observed, with more rainfall over the Indian peninsula, than in the monsoon zone (e.g. GSFC in Fig. 8). In a third group, the primary rainbelt is over the equatorial Indian ocean with very little rainfall over most of the Indian region (e.g. UGAMP in Fig. 8). We

have therefore classified the models on the basis of the simulated rainfall over the Indian monsoon zone into categories A, B and C. In this classification, the relative strengths over the peninsula to the south of the monsoon zone and the equatorial Indian Ocean have also been considered. The rainfall over the Indian monsoon zone and the ratios of the rainfall (2) over the peninsula, south of the monsoon zone, and (2) over the equatorial Indian ocean, to that over the Indian monsoon zone in different models are shown in Table 3. The class (I or II) to which the model has been assigned on the basis of the simulation of the seasonal migration over the Asia-Pacific sector, as well as the pattern correlation coefficient with the observed July–August rainfall for the region 70 °E–90 °E; 0–30 °N are also indicated in Table 3.

The mean rainfall pattern for July–August simulated by the different models are shown in Fig. 9. It is clear that models of category A represent the rainfall pattern and particularly the monsoon rainbelt in a reasonably realistic manner. The simulation of the mean rainfall pattern by NCEP2 appears to be the most realistic and is better than that of NCEP1 over the Indian region. Table 3 shows that classes I, II are almost equally represented in this category A. However, as noted in Sect. 3.3, for the models of class II in category A (e.g. COLA, MGO etc.), the rainfall over the Indian monsoon zone is associated with a secondary precipzone largely restricted to these longitudes, whereas for those in class I it is associated with a planetary scale system. There are differences in the skill of simulation of the other rainbelts. For example, in the GFDL simulation the oceanic rainbelt (II) is absent in the mean pattern (although it does occur in some years). In the MPI simulation, the oceanic rainbelt II is as intense as the continental one (rainbelt I), and the orographic rainbelts III and IV are missing. Note that, for the models in the subset A_1 (A_2), the mean rainfall over the Indian

Table 3 Observed and Simulated July–August mean rainfall (mm/day) over the monsoon zone (15 °N–25 °N), ratios of mean rainfall over the peninsula (PEN, 7.5 °N–15 °N) and equatorial Indian Ocean (EIO, 5 °S–5 °N; 67.5°–85 °E) to mean rainfall over the monsoon zone (MNS), category of the mean July–August rainfall pattern over the Indian region, the class from Table 2 and the class based on SP test (Sect. 5.1)

Models	Mean Rainfall (MNS)	Ratios PEN/MNS	Ratios EIO/MNS	Category	Classes	SPtest	Correlation coefficient
IMD (observations)	7.5	0.7	0.7				
CNRM	6.3	0.8	0.8	A_1	I	F	0.59
CSIRO	11.0	0.6	0.6	A_1	I	P	0.46
GFDL	8.7	0.7	0.2	A_1	I	P	0.39
NCEP2	7.0	0.9	0.6	A_1	I	–	0.58
JMA	8.2	0.9	0.5	A_1	II	F	0.51
MGO	15.8	0.4	0.2	A_1	II	P	0.45
MPI	5.6	0.5	1.6	A_2	I	F	0.01
NCEP1	6.2	0.8	1.1	A_2	II	F	0.51
COLA	4.2	0.9	2.0	A_2	II	F	0.30
ECMWF	4.6	0.6	2.3	A_2	II	P	−0.06
NRL	6.5	0.9	1.4	A_2	II	P	0.36
BMRC	9.3	1.1	0.5	B_1	I	P	0.67
GISS	7.9	1.7	0.6	B_1	I	P	0.46
GLA	5.7	2.5	0.2	B_1	I	P	0.49
GSFC	7.9	1.4	0.4	B_1	I	P	0.47
MRI	9.9	1.3	0.4	B_1	I	P	0.18
UKMO	7.6	1.1	0.8	B_1	I	P	0.60
DNM	9.0	1.6	0.1	B_1	II	F	0.60
RPN	7.2	1.8	1.5	B_2	I	F	0.18
CSU	6.2	1.3	2.6	B_2	II	P	−0.19
YONU	4.5	1.4	2.6	B_2	II	F	−0.07
DERF	1.3	3.8	10.6	C_1	II	F	−0.39
IAP	0.9	10.9	12.2	C_1	II	P	−0.30
LMD	2.4	2.2	7.0	C_1	II	P	−0.18
NCAR	2.5	3.0	6.1	C_1	II	F	−0.38
SNG	2.9	0.4	2.0	C_1	II	P	0.07
SUNYA	2.0	1.9	2.5	C_1	II	F	−0.16
UCLA	6.5	0.7	2.0	C_1	II	F	−0.05
UGAMP	0.4	7.5	47.3	C_1	II	P	−0.24
UIUC	2.5	3.7	3.1	C_1	II	F	−0.19
CCC	4.6	0.8	1.1	C_2	I	F	0.05

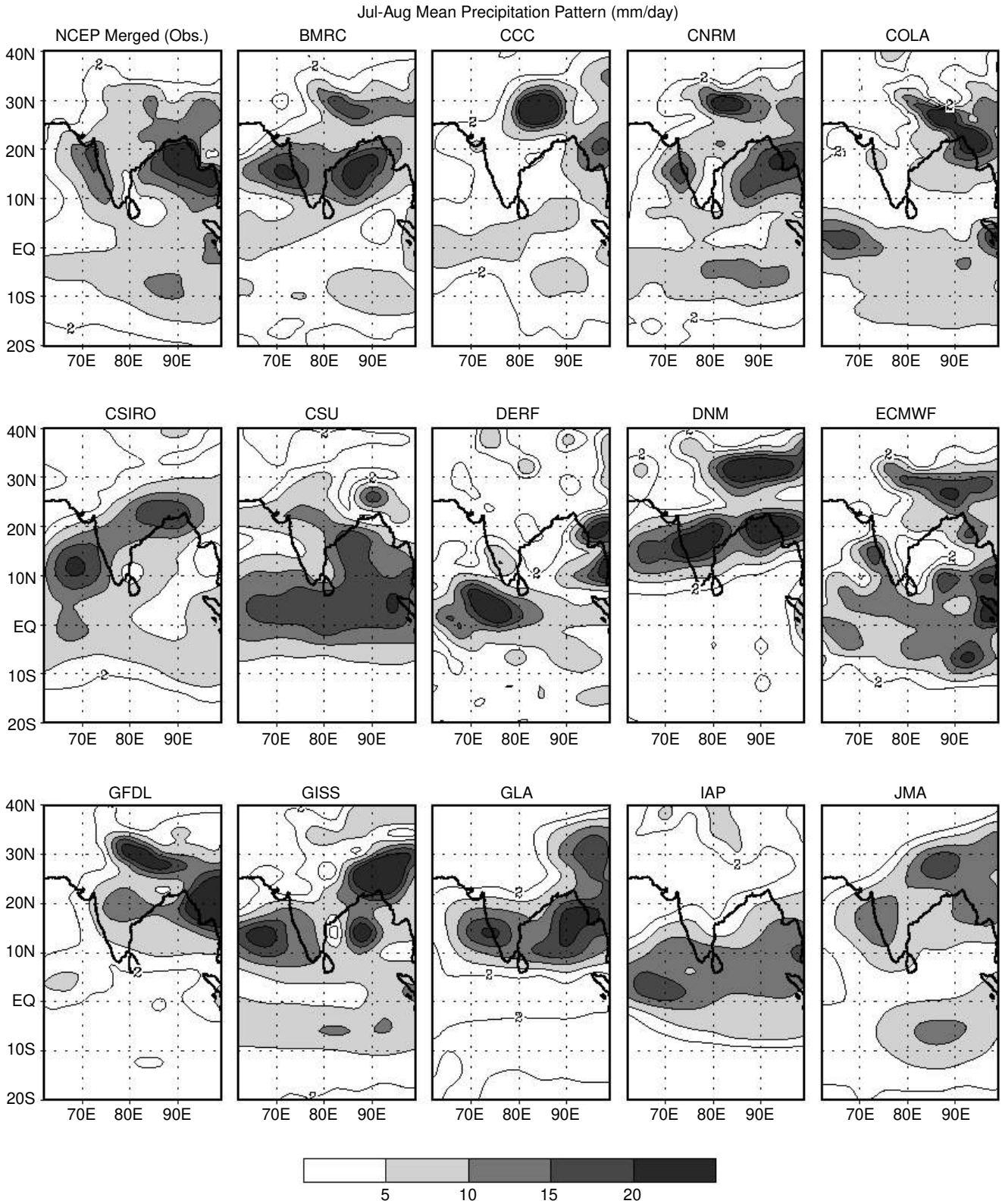

Fig. 9 Simulation of the mean July–August precipitation over the Indian region

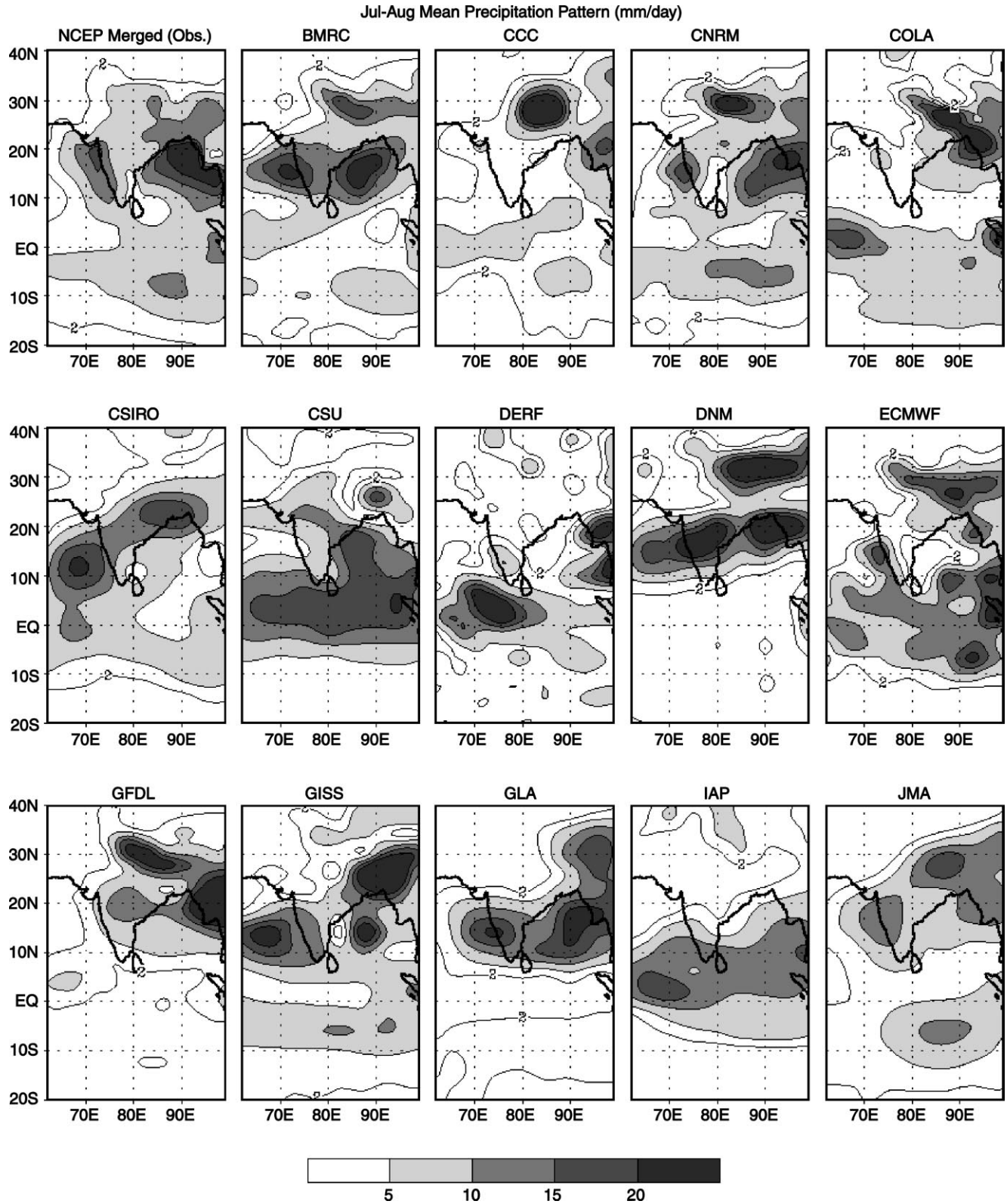

Fig. 9 (*Continued*)

monsoon zone is larger (smaller) than that over the equatorial Indian Ocean. Nevertheless, we have assigned all these models to category A because more weight is given to the realistic simulation of the rainbelt over the monsoon zone than to the relative intensity of the oceanic rainbelt. Since no such bias comes into the calculation of the pattern correlation coefficient, the coefficient for some models belonging to A_2 is much smaller than that of models in A_1 (Table 3).

In models of category B (such as UKMO and GSFC), the maximum rainfall over the Bay of Bengal occurs southward of the observed maximum, over the head of the Bay, and a prominent zonal rainbelt occurs around 15 °N, stretching across from the Arabian sea (near the orographic rainbelt IV), across the Indian peninsula and the Bay of Bengal and beyond over the West Pacific. Thus, the southward location of the primary rainbelt vis a vis the observations is the distinguishing attribute of category B. In addition, in some models such as the UKMO model, the orographic rainbelt (III) is simulated. The isohyets in this case are realistic in the northwestern part, whereas they tend to be zonal in the models, such as GSFC, without the rainbelt III. However in the UKMO model, there is a narrow zonal belt with relatively little rainfall over the Indian monsoon zone, in the 'no man's land' between this rainbelt and the major zonal rainbelt around 15 °N. In the simulations of these models, relatively low rainfall over the monsoon zone and the unusually high rainfall over the peninsula (particularly near the east coast) are unrealistic features. For models of category B_1 (B_2) the rainfall over the equatorial Indian ocean is smaller (larger) than that over the Indian monsoon zone. Whereas the pattern correlation coefficient of models of category B_1 is comparable to that of the models of category A_1, that of category B_2 is very small.

For the models in category C, the prominent rainbelt is either over the equatorial Indian Ocean (C_1) or close to the orography to the north of the Indian monsoon zone (C_2). There is hardly any rainfall over the Indian monsoon zone in the simulation of C_1. In the CCC simulation (category C_2), the orographic rainbelt spreads, to some extent, over the Indian monsoon zone resulting in some rainfall over this region. Note that the pattern correlation coefficient for all the models in category C is very small or negative.

We note that a realistic simulation of the rainfall pattern over the Indian monsoon zone has been achieved by models which simulate a seasonal migration of the primary rainbelt, as well as those in which a secondary zone occur over the region (i.e. classes I and II). Note that the categorisation into A and B is based mainly on the latitudinal location of the primary rainbelt over the Indian region. Of these, models of categories A_2 and B_2 simulate relatively high rainfall over the equatorial oceans. The mean rainfall, for the region as a whole, simulated by models of categories A_1 and B_1 is more realistic, with reasonable rainfall distribution over the continent and high values of pattern correlation. Most of the models of categories A_1 and B_1 belong to class I (10 out of 13). On the other hand, the simulated mean rainfall over the monsoon zone is less than observed for category C and the majority of the models in this category belong to class II. The mean July–August rainfall pattern of class I models is better correlated with the observed than that of class II models (0.64, 0.06 respectively, Fig. 10).

4.2 Implications

Whereas almost all the models simulate adequately the seasonal variation of the ITCZ over the African region, over the Indian longitudes a large fraction of the models show the ITCZ as a persistent feature over the equatorial Indian ocean in all seasons (with a secondary convergence zone over the Indian monsoon zone in some). It has been pointed out that this region has two favourable locations for the tropical convergence zones, one over the heated subcontinent, and another over the warm waters of the equatorial Indian ocean (Sikka and Gadgil 1980; Gadgil et al. 1992). In nature, although the continental TCZ is dominant, the oceanic TCZ appears intermittently throughout the summer leading to a bimodal latitudinal profile. On the other hand, many models seem to have a tendency to get locked into either the oceanic or the continental mode.

We have noted that reasonably realistic mean rainfall patterns of July–August are produced by some models, with realistic seasonal migration of the TCZ over the Asia West Pacific sector (class I), as well as some models of class II, for which the system responsible for the Indian monsoon rainfall is more localised and does not stretch across East Asia and the West Pacific. In all models of class I, the primary rainbelt is north of 10 °N in the summer monsoon over the Indian region, with relatively little precipitation in the equatorial region (10 °S–10 °N). In all models of class II, there is a major rainbelt over the equatorial Indian ocean.

The two sets of models (classes I and II) support different hypotheses about the system responsible for the monsoon. Since Halley (1686), the monsoon has been viewed as a gigantic land-sea breeze. Land–ocean temperature contrast has been considered to be the most important factor in generating the monsoon circulation and rainfall. Alternatively, the monsoon has been considered as a manifestation of the seasonal migration of the planetary scale equatorial trough (Riehl 1954, 1979), near-equatorial trough (Ramage 1971) or the intertropical convergence zone i.e. the ITCZ (Charney 1969). Studies of the daily variation of the maximum cloudiness zone, from satellite imagery, and the monsoon trough at 700 hPa, suggest that the large-scale monsoon rainfall over the Indian region is

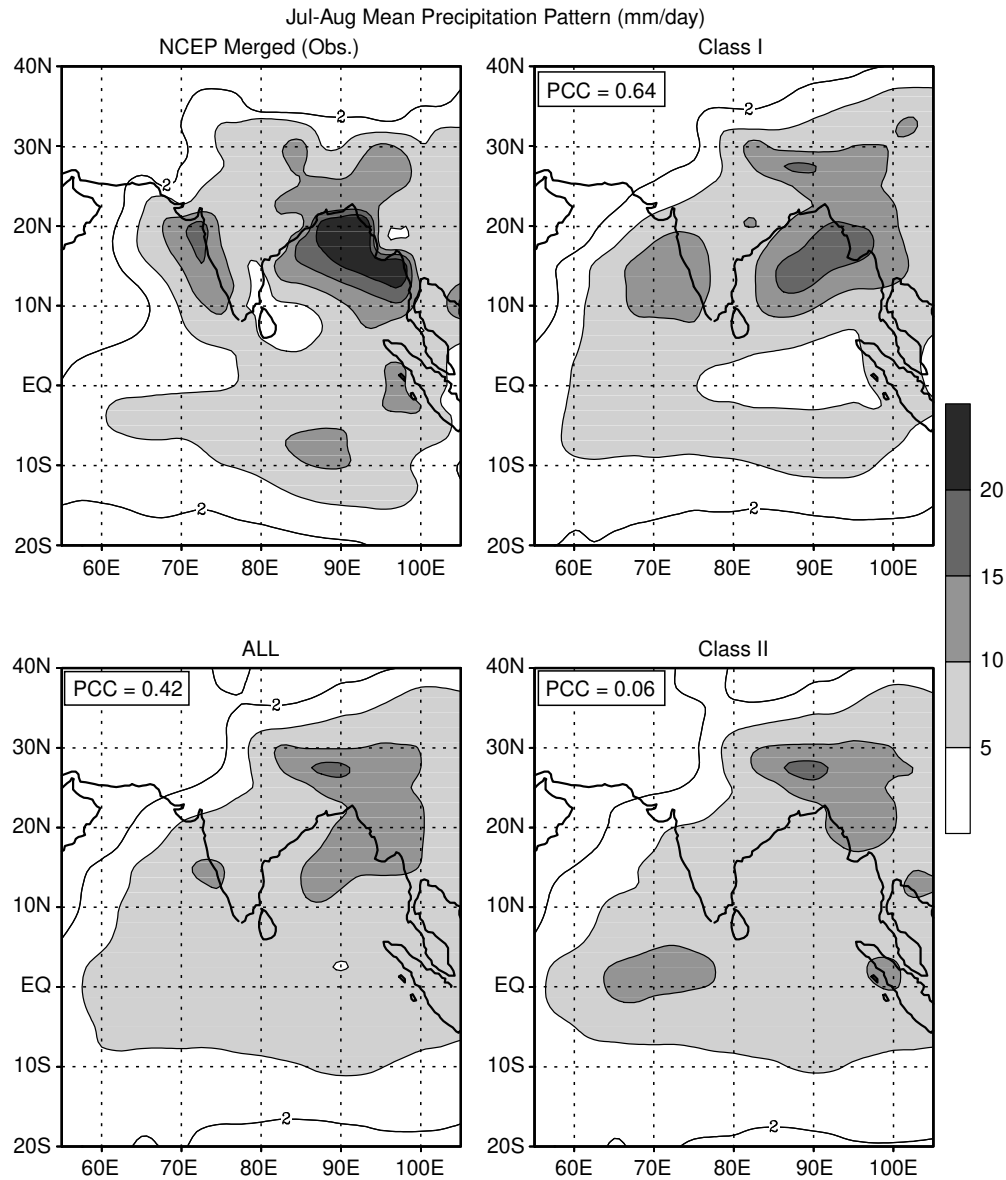

Fig. 10 Observed and simulated mean July-August precipitation over the Indian region. Observation (*top left*), average of all AMIP models (*bottom left*), average of models of class I (*top right*) and average of models of class II (*bottom right*). The *pattern correlations* with observed data for the region 70 °E–90 °E; 0–30 °N, based on 2.5° common grid are given in the *top left* of each model panel

associated with the migration of the ITCZ over the heated subcontinent in the summer (Sikka and Gadgil 1980; Gadgil 1988). The models of class I, therefore, appear to be more realistic. Although there are some lacunae in the simulations of the models of category B in class I relative to those of category A within this class, we believe that they are closer to reality than the models of class II, category A, because they simulate more realistically the seasonal migration of the planetary scale ITCZ and, hence, the structure of the planetary scale monsoon.

There appears to be no systematic relationship between which of the two classes I and II, the simulation of a model belongs and the way important physical processes such as convection and hydrology are parametrised. Typically, about half of the models adopting a particular convective scheme belong to class I. If we consider the simulation of the large-scale monsoon rainfall over the Indian region, category A comprises models with every type of convective parametrisation. This is not surprising, because it is known that the category, to which the monsoon simulation of a model belongs, is dependent on various factors including physical parametrisation as well as numerics and, hence, on a particular version. At any point in time such as during the AMIP runs, in a significant fraction of the models, the rainbelt II on the equatorial Indian ocean dominates the monsoon rainbelt. The transition from such a simulation to one in which the continental TCZ dominates and vice versa can occur with change in physics or numerics (e.g. Laval et al. 1996; Sperber et al. 1994).

5 Interannual variation of all-india summer monsoon rainfall

The importance of generating predictions of the summer monsoon rainfall over India cannot be overemphasised because the fortunes of this densely populated country are known to fluctuate with the monsoon. In years with large positive (negative) anomalies of the monsoon rainfall the foodgrain production is larger (smaller) by 10 to 20% on the all-India scale (Parthasarathy et al. 1992). It is, therefore, of interest to assess the skill of the models in simulating the interannual variation of the summer monsoon rainfall, particularly for good and deficient monsoon years. The Indian region has had a large network of well-distributed observatories for over a century and the rainfall data have been carefully compiled and extensively analysed. Hence, it is worthwhile to compare simulations of models with the observations of mean patterns or interannual variation which are considered to be very reliable. It should be noted that the skill in the AMIP runs can be considered to be a measure of the potential skill, since the models have been driven with the observed boundary conditions over the oceans.

All-India summer monsoon rainfall for each model has been estimated as the total rainfall over the grids indicated in Fig. 11. The mean and standard deviation of the all-India summer monsoon rainfall during the AMIP decade, are shown in Table 4 for each model. Clearly many models simulate the mean all-India monsoon rainfall reasonably well. As expected, the simulated mean for the models in category C_1 with most of the rainfall over the equatorial Indian ocean is less than observed, particularly so when they do not simulate the orographic rainfall near the northern boundary. Note that there is considerable variation in the simulated amplitude of the interannual variation. The coefficient of variation which is observed to be about 10%, varies from 4% for the CSIRO model to 24% for the ECMWF model and 29% for MPI even within the class of models with realistic mean patterns! We next compare the anomalies of the seasonal rainfall (from the model mean, normalised by its own standard deviation) during the AMIP decade with the observed.

The observed variation of the all-India monsoon rainfall during the AMIP decade is shown in Fig. 12 (top panel). There are seven monsoon seasons with anomalies greater than half the standard deviation, with a negative anomaly in 1979, 1982, 1986, 1987 and a positive anomaly in 1980, 1983, 1988. We note that the mean summer monsoon rainfall of 81.8 cms and the standard deviation of 9.8 cms are different (lower and higher respectively) from the longer-term mean of 85.2 cms and standard deviation of 8.5 cms (Parthasarathy et al. 1994). Thus, although the season of 1986 has an anomaly of amplitude larger than one standard deviation with respect to the long-term values, the magnitude of the anomaly from the AMIP mean is 0.73 of the AMIP standard deviation. Hence, in this analysis we take anomalies with amplitude greater than half the standard deviation for the AMIP decade to be significant, and a line, indicating the value of half the standard deviation, is also indicated in Fig. 12. The interannual variation of the simulated anomaly of the all-India average rainfall during the AMIP decade for a few representative models is also shown in Fig. 12. Although, we have not used a land-sea mask specifically tailored to isolate the inland borders of India as done by Sperber and Palmer (1996), the anomalies obtained by us are consistent with those of Sperber and Palmer (1996) (Sperber 1997, personal communication). Most of the models are unable to capture all the fluctuations of the monsoon rainfall on the interannual scale in the AMIP decade as shown by Sperber and Palmer (1996). In fact the only model which simulates deficient rainfall, with amplitude of anomaly greater than half the standard deviation in 1979, 1982, 1986 and 1987 is the GLA model and the only model which simulates significant positive anomalies in 1980, 1983 and 1988 is the CSIRO model. Even four of these events are simulated by very few models.

It is also important to note that the maximum positive or negative anomalies in models often occur in years in which the observed monsoon rainfall was near normal or had an anomaly of the opposite sign. For example, in the ECMWF model, the maximum rainfall occurs in 1980 and minimum in 1985; in the GFDL simulation the largest excess occurred in 1982 and the minimum rainfall in 1984.

We first consider the simulation of the seven monsoon seasons with significant anomalies. We note that of these seven seasons, only two deficient seasons i.e. 1982, 1987 and two good monsoon seasons i.e. 1983, 1988 were associated with ENSO. We discuss the simulations for these four seasons in Sect. 5.1 and its relation to the simulation of mean pattern in Sect. 5.2. Analysis of the simulation of the other three seasons i.e. 1979, 1980, 1986 is given in Sect. 5.3. The overall skill of simulation of interannual variation in the AMIP decade is discussed in Sect. 5.4.

5.1 Monsoon seasons with ENSO links

Since in the AMIP all the models were run with the observed SST, we expect the events associated with major variations of the SST field, such as the ENSO, to be well simulated. It is well known that there is a correspondence between deficit (excess) in the Indian monsoon rainfall and the occurrence of warm events/El Niño (cold events/La Niña) in the Pacific (Sikka 1980; Rasmusson and Carpenter 1983; Ropelewski and Halpert 1987, 1996 etc.). Thus, there is some basis to expect reasonable skill in the simulation of the deficit/excess fluctuations associated with the ENSO.

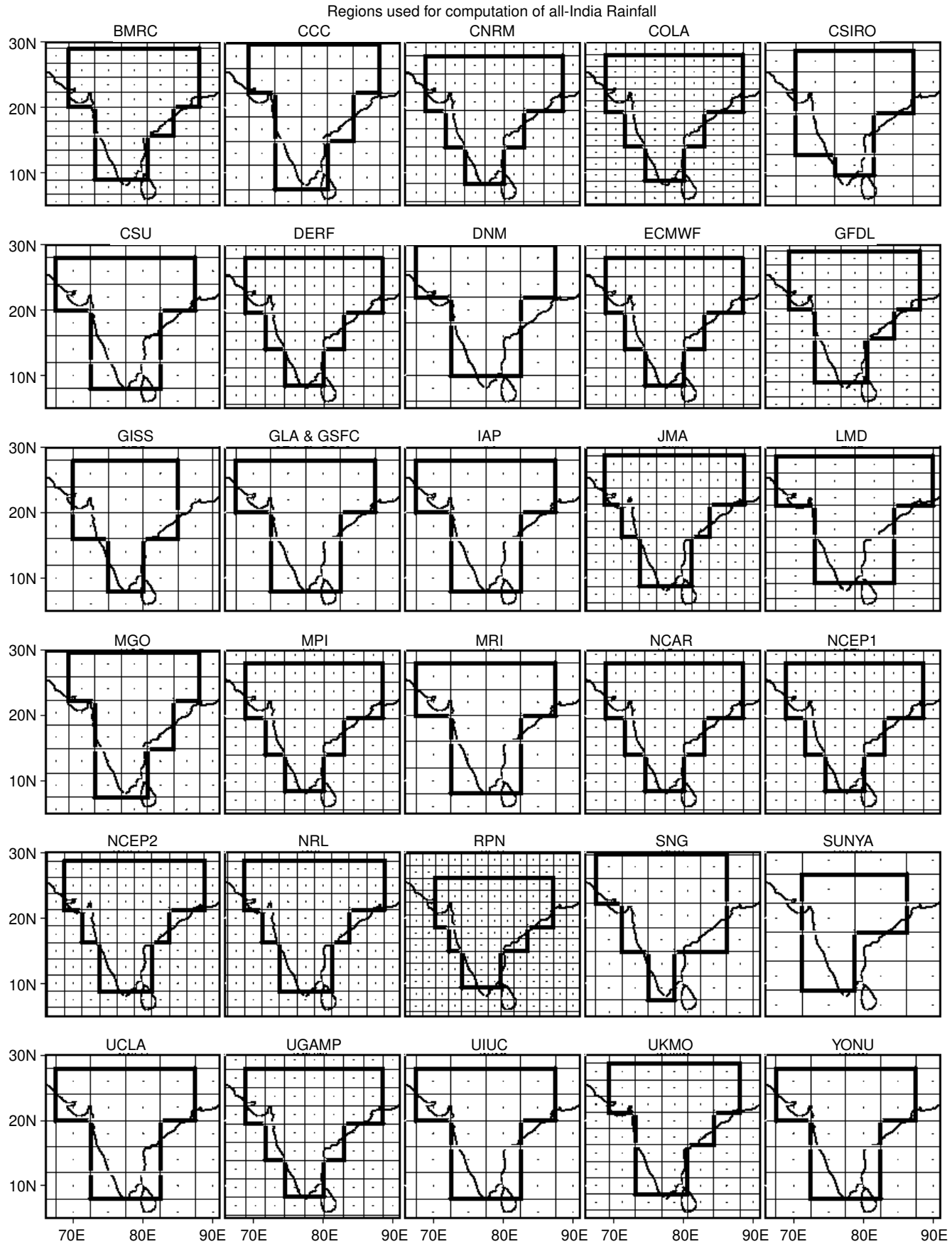

Fig. 11 Region considered for computation of all-India summer monsoon rainfall for different models

Table 4 Observed and simulated mean, standard deviation (mm/day) and coefficient of variation of the all-India summer monsoon (June–September) rainfall

Models	Mean	σ	$(\sigma/\text{mean}) \times 100$
IMD (observations)	6.48	0.86	13.3
BMRC	9.00	1.24	13.7
CCC	6.68	0.41	6.1
CNRM	6.02	0.91	15.1
COLA	5.91	0.90	15.2
CSIRO	7.89	0.33	4.2
CSU	7.15	0.49	6.9
DERF	2.33	0.88	37.6
DNM	8.73	0.99	11.4
ECMWF	4.09	0.98	23.9
GFDL	6.68	1.12	16.8
GISS	5.40	1.48	27.5
GLA	5.43	1.16	21.4
GSFC	7.81	0.52	6.6
IAP	2.72	0.33	12.0
JMA	8.57	0.65	7.6
LMD	3.42	0.98	28.6
MGO	12.48	0.30	2.4
MPI	4.03	1.18	29.2
MRI	10.09	0.99	9.8
NCAR	4.57	0.86	18.7
NCEP1	5.15	1.49	28.9
NCEP2	8.49	1.20	14.2
NRL	6.62	0.50	7.6
RPN	7.50	0.87	11.6
SNG	3.45	0.99	28.7
SUNYA	2.05	0.51	24.8
UCLA	5.56	0.24	4.4
UGAMP	1.90	0.49	25.8
UIUC	3.38	0.68	20.0
UKMO	7.00	0.47	6.8
YONU	4.72	0.91	19.3

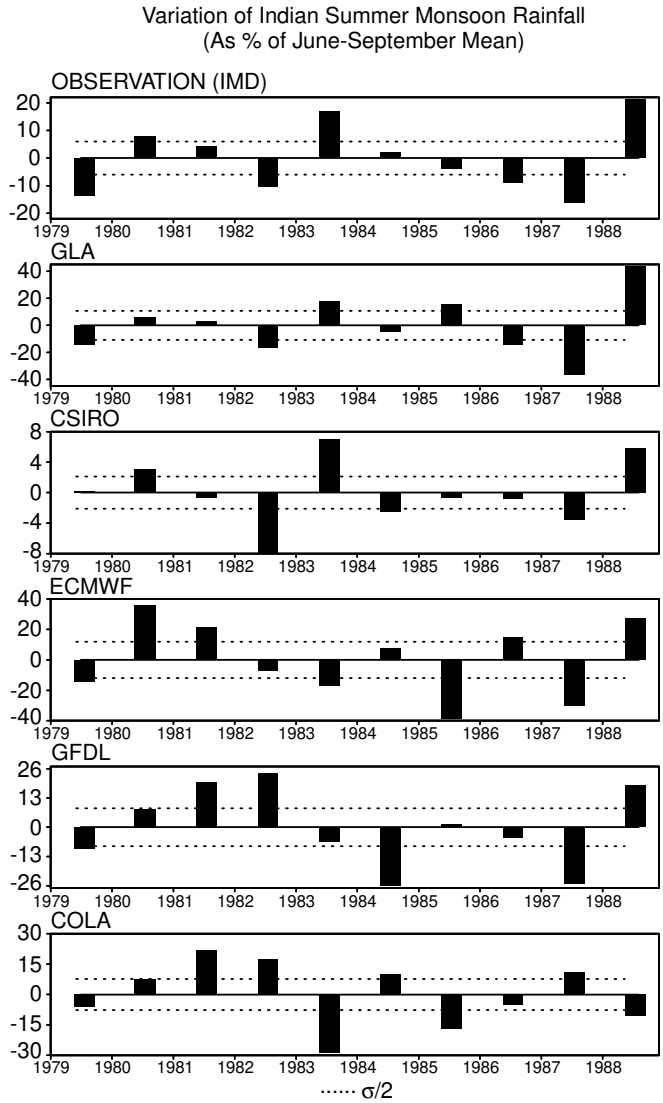

Fig. 12 Observed and model simulated variation of all-India summer monsoon rainfall

Palmer et al. (1992) have shown that the SST anomalies over the Pacific play an important role in generating the interannual variation of the Indian monsoon. The all-India monsoon rainfall is highly correlated with the SST of the Central Pacific (Lau and Yang 1996, and references therein). Lau and Yang's (1996) analysis of Indian rainfall and SST over the Pacific indicates a strong simultaneous correlation of the summer monsoon rainfall with SST in the region 170 °W–150 °W; 5 °S–5 °N (their Fig. 2a), which is a part of the NINO4 region. The observed SST anomalies over this part of Central Pacific during the AMIP decade are shown in Fig. 13. This shows that while the warm event commencing in early 1982 ended in the middle of the summer monsoon season of 1983, the second warm event of 1987 ended in early 1988, well before the summer monsoon season. The variation of the precipitation anomaly over the Central Pacific (also shown in Fig. 13) is seen to be directly related to the SST as first pointed out by Bjerknes (1969). Thus, the atmospheric teleconnection of the Indian monsoon with the Pacific involves association of large positive (negative) precipitation anomalies over the Central Pacific with large deficits (excess) of the Indian monsoon rainfall.

Of the four seasons of deficient/excess rainfall in the AMIP period, the droughts of 1982 and 1987 were associated with El Niño, and the season of 1988 with La Niña. The El Niño retreated half way through the season of 1983 which turned out to be a good one with bountiful rainfall. Hence, we consider the simulation of the monsoon seasons of 1982, 1987 (droughts) and 1988 (good monsoon) which were associated with ENSO. We consider separately the season of 1983, which many models could not simulate, perhaps because (as seen in Fig. 13) the SST and rainfall anomalies over the Central Pacific associated with the El Niño reversed in August i.e. right in the middle of the summer monsoon.

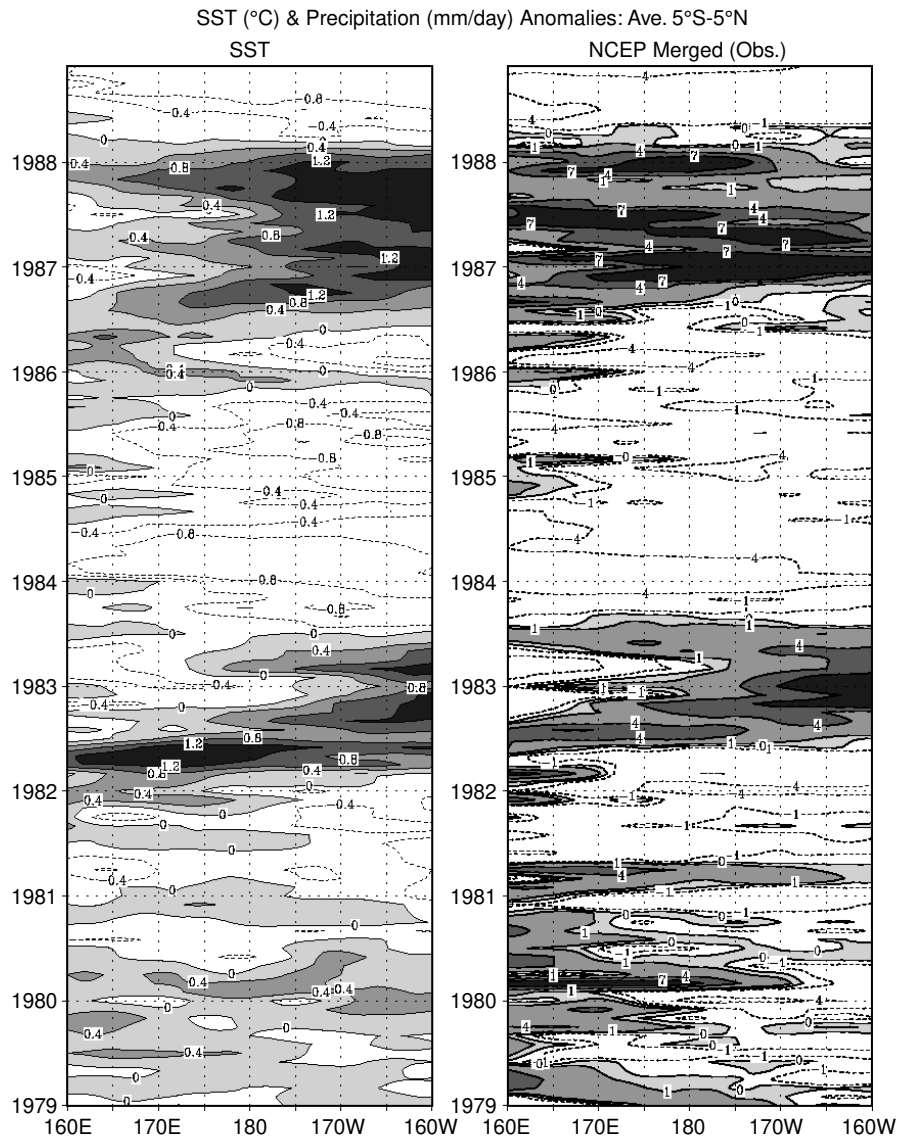

Fig. 13 Variation of the anomalies of SST and precipitation (averaged over 5 °S–5 °N) over the Central Pacific

We first consider the simulation of the precipitation anomalies over the Central Pacific during the summer monsoon seasons of 1982, 1987 and 1988 (Table 5). It is seen that 29 out of the 31 simulations captured the variation of the precipitation anomaly over the Central Pacific; in only two simulations is the anomaly negligible, or of the wrong sign, in one or more of these seasons.

The observed and simulated anomalies of all-India monsoon rainfall for the seasons of 1982, 1987 and 1988 are given in Table 6a and for the season of 1983 in Table 6b. The class to which the models belong, on the basis of simulation of the seasonal variation of the Asia West Pacific sector (Table 2), is also indicated. Sperber and Palmer (1996) documented success/failure of models in simulating qualitatively the rainfall/ENSO SST teleconnection pattern (henceforth referred to as SP test). In the last column of Table 6, whether the model passed or failed to simulate the teleconnection pattern, i.e., the SP test (from Fig. 1c of Sperber and Palmer 1996) is indicated by P and F respectively. A measure of the skill of simulation of the four monsoon seasons of each model is the score given in Table 6. For each season, the score is $+2$ (-2) if the amplitude of the anomaly is greater than half the standard deviation of the model, and the anomaly is of the same (opposite) sign as observed. If the amplitude of the anomaly is less than half the standard deviation of the model, the score is taken as $+1(-1)$ if the sign of the anomaly is the same (opposite) to that of the observed. Thus the square of the error (ε^2) in simulation of each event varies from 0 to 4. The average error, defined as the square root of the ratio of the sum of the errors (ε^2 for all the events) and the number of events, is also shown in Table 6. Table 6a shows that 11 models simulate anomalies of the correct sign; of these, in the first five

Table 5 Observed and simulated anomalies of June–September precipitation over the Central Pacific (170 °W–150 °W; 5 °S–5 °N, expressed as percentage of mean precipitation) and coefficient of variation

Models	1982	1987	1988	$(\sigma/\text{mean}) \times 100$
NCEP (observations)	56.7	93.3	−70.0	48.4
BMRC	26.3	53.9	−52.6	28.8
CCC	41.9	106.5	−51.6	43.1
CNRM	23.2	66.1	−78.6	36.9
COLA	4.1	30.6	−34.7	16.2
CSIRO	34.9	82.5	−73.0	40.0
CSU	21.0	50.6	−55.6	26.9
DERF	24.2	93.9	−45.5	36.4
DNM	11.1	33.3	−30.6	15.8
ECMWF	50.0	162.5	−91.7	73.4
GFDL	54.3	122.9	−65.7	53.6
GISS	54.8	78.6	−47.6	38.7
GLA	76.0	112.0	−56.0	56.9
GSFC	19.0	54.8	−50.0	28.0
IAP	31.5	46.3	−51.9	28.6
JMA	20.8	72.9	−37.5	31.1
LMD	12.2	104.1	−53.1	40.2
MPI	89.5	278.9	−84.2	105.3
MRI	38.1	66.7	−35.7	29.3
NCAR	89.5	210.5	−63.2	81.5
NCEP2	64.4	54.2	−66.1	38.9
NRL	104.5	118.2	−81.8	60.7
RPN	10.2	35.6	−13.6	15.3
SNG	36.1	161.1	−61.1	60.0
SUNYA	18.0	80.3	−34.4	31.0
UCLA	28.3	83.3	−48.3	34.3
UGAMP	79.3	75.9	−96.6	73.9
UIUC	18.6	53.5	−44.2	24.8
UKMO	73.9	204.3	−82.6	82.0
YONU	68.6	9.8	−27.5	32.6
MGO	−2.7	2.7	−27.4	16.6
NCEP1	−17.5	−3.5	0.0	12.3

the amplitude is greater than half the standard deviation (of the model). In the three models at the bottom of Table 6a the simulated anomalies are of the opposite sign to the observed, for all the three seasons! The average error ranges from 0 to 4. We note from Table 6b that, as expected, the error is high in a larger number of models in the simulation of the anomaly of the season of 1983.

For 1982, 1987, 1988, in spite of the fact that in 29 out of 31 simulations, the precipitation anomalies over the Central Pacific were of the same sign as observed for each of the three seasons, the anomalies over the Indian region are not simulated by several models, suggesting that there are some lacunae in the simulation of the teleconnection with the Pacific. Note the marked improvement in the simulation of the interannual variation of the NCEP2 (class I) vis a vis NCEP1 (class II). Whereas NCEP1 could not simulate the local response over Central Pacific, the NCEP2 simulated it for all the events. Further, NCEP1 simulated anomalies of the correct sign in 1982, 1988 for all-India monsoon rainfall (although over the Central Pacific the anomaly was of the opposite sign to observed in 1982 and negligible in 1988) and an anomaly of opposite sign to that observed in 1987 (when the response over the Central Pacific was also of opposite sign to that observed). On the other hand, the NCEP2 simulated the anomalies over the Central Pacific as well as of the Indian monsoon for all the three events as observed. Thus, the local response over the Central Pacific, as well as the teleconnection to the all-India monsoon rainfall, have improved markedly and became realistic in NCEP2.

It is seen from the last column of Table 6a that all the five top models and nine of the top ten models pass the SP test for the teleconnection pattern and nine of the bottom ten fail to do so. Thus, the performance of the models in simulating the variation during the seasons of 1982, 1987 and 1988 is directly related to the Sperber and Palmer (1996) criterion based on performance in simulating the teleconnection pattern. However, there are exceptions, with JMA simulating the interannual variation correctly despite failing the test and LMD not simulating despite passing the test.

Further insight into the performance of the models in simulating the interannual variation of the Indian monsoon rainfall can be gained by considering the membership of classes I and II (Table 2). Note that four of the five models on top of Table 6a belong to class I (i.e. with realistic simulation of the seasonal migration over the Asia-Pacific region) and six of the seven models at the bottom of the Table 6a belong to class II. It therefore appears that the probability of simulating the interannual variation is larger for models belonging to class I. Consider the frequency distribution of the total error separately for the classes I and II (Fig. 14). The difference in the performance of these two classes in simulating the anomalies of the all-India monsoon rainfall for three major events is clearly brought out. Additional intercomparisons of different versions of the same model (which may become possible with the runs of AMIP II) are needed to test this hypothesis further.

It is interesting that two independent approaches to classification of model simulations have proved to be useful. There is a very close correspondence between the performance of the models in simulating the interannual variability during the ENSO years, and their ability to simulate the teleconnection pattern used as criterion for classification by Sperber and Palmer (1996). As noted alredy there is also a large difference in the skill of simulation of the interannual variation of all India monsoon rainfall between the models of the two classes (I and II) identified here on the basis of seasonal migration of the rainbelt. Since this criterion, based on seasonal mean patterns, differs from the criterion used by Sperber and Palmer (1996) based on the pattern of teleconnection of interannual variation, this set of classes is not identical to the classes derived by Sperber and Palmer (1996). Of the 30 models common to their

Table 6a Observed and simulated anomalies of all-India summer monsoon (June–September) rainfall (normalised with half the standard deviation), score for each event, average error, the class from Table 2 and the class based on SP test

Models	1982		1987		1988		$\sqrt{\{(\Sigma\varepsilon^2)/3\}}$	Classes	
	Anomaly	Score	Anomaly	Score	Anomaly	Score			SPtest
IMD (observations)	−1.70	2	−2.65	2	3.51	2			
CSIRO	−3.76	2	−1.72	2	2.79	2	0.0	I	P
GISS	−1.31	2	−1.86	2	1.05	2	0.0	I	P
GLA	−1.54	2	−3.44	2	4.07	2	0.0	I	P
MRI	−1.63	2	−2.64	2	3.01	2	0.0	I	P
NRL	−3.26	2	−1.58	2	3.11	2	0.0	II	P
BMRC	−2.98	2	−2.09	2	0.32	1	0.58	I	P
GSFC	−4.01	2	−0.58	1	2.65	2	0.58	I	P
ECMWF	−0.61	1	−2.53	2	2.30	2	0.58	II	P
NCEP2	−0.63	1	−1.37	2	0.18	1	0.82	I	–
JMA	−2.55	2	−0.63	1	0.19	1	0.82	II	F
UGAMP	−0.30	1	−3.77	2	0.13	1	0.82	II	P
SNG	0.29	−1	−2.81	2	1.32	2	1.73	II	P
UIUC	0.61	−1	−0.08	1	1.40	2	1.83	II	F
GFDL	2.83	−2	−2.97	2	2.22	2	2.31	I	P
MPI	−2.41	2	2.83	−2	1.66	2	2.31	I	F
UKMO	2.53	−2	−3.33	2	1.28	2	2.31	I	P
CNRM	−0.23	1	2.27	−2	2.84	2	2.38	I	F
NCEP1	−0.43	1	1.32	−2	1.23	2	2.38	II	F
CSU	1.87	−2	−0.81	1	2.67	2	2.38	II	P
IAP	2.73	−2	−2.64	2	0.76	1	2.38	II	P
MGO	2.78	−2	−3.01	2	0.22	1	2.38	II	P
UCLA	−0.92	1	3.33	−2	3.77	2	2.38	II	F
YONU	2.85	−2	−0.56	1	1.44	2	2.38	II	F
CCC	3.17	−2	−0.79	1	0.55	1	2.45	I	F
DERF	−0.04	1	2.26	−2	−0.92	−1	2.94	II	F
NCAR	4.52	−2	−0.26	1	−0.79	−1	2.94	II	F
LMD	3.81	−2	−3.13	2	−1.55	−2	3.27	II	P
DNM	2.63	−2	1.44	−2	0.83	1	3.32	II	F
SUNYA	3.06	−2	0.63	−1	−0.50	−1	3.37	II	F
RPN	0.54	−1	2.05	−2	−1.19	−2	3.70	I	F
COLA	2.27	−2	1.44	−2	−1.40	−2	4.00	II	F

study and the present study, 16 (14) pass (fail) the SP test. Whereas a majority of the models that fail the test belong to class II (10 out of 14); half of the models that pass the test belong to each class. Similarly, whereas a larger fraction of models of class I (8 : 4) pass the test, the number of models of class II that fail (10) is only slightly larger than the number that passed (8).

5.2 Simulation of mean versus simulation of interannual variation

We have seen that the skill of simulation of interannual variation of the Indian summer monsoon rainfall for the ENSO associated seasons is higher for the class of models that simulate the observed teleconnection pattern (i.e. pass the SP test) than for the class of models that fail to do so. Sperber and Palmer (1996) showed that the mean seasonal rainfall pattern of the models that pass the SP test is better correlated with observations than that for the class of models that fail the test (correlation coefficients of 0.68 and 0.47 for the region 70 °E–90 °E; 0–30 °N) and suggested that "a good rainfall climatology and proper simulation of interannual variability are associated".

We have shown that the interannual variation for ENSO associated monsoon seasons is also better simulated by models of class I (with a realistic simulation of the seasonal migration of the rainbelt over the Asia West Pacific region), than those of class II. It was shown in Sect. 4.1 that the pattern correlation coefficient of mean July-August rainfall with the observed mean rainfall is higher for models of class I than that for models of class II (Fig. 10). We find that the mean June-September rainfall pattern of models of class I is also much better correlated with the observed pattern than that of class II with pattern correlation coefficients 0.71, 0.25 respectively. These results support Sperber and Palmer's (1996) hypothesis of association between better simulation of interannual variability of Indian summer monsoon rainfall and better simulation of the mean pattern.

However, it is important to note that the pattern correlation coefficients of the models of each class have

Table 6b Observed and simulated anomalies of all-India summer monsoon (June-September) rainfall (normalised with half the standard deviation), score for the event, average error, the class from Table 2 and the class based on SP test

Models	1983 Anomaly	Score	$\sqrt{\{\Sigma\varepsilon^2\}}$	Classes	SPtest
IMD (observations)	2.80	2			
CNRM	2.17	2	0.0	I	F
CSIRO	3.33	2	0.0	I	P
CSU	1.22	2	0.0	II	P
DNM	2.05	2	0.0	II	F
GLA	1.68	2	0.0	I	P
GSFC	1.48	2	0.0	I	P
MGO	2.69	2	0.0	II	P
NCAR	1.88	2	0.0	II	F
DERF	0.31	1	1.0	II	F
RPN	0.25	1	1.0	I	F
SUNYA	0.47	1	1.0	II	F
UCLA	0.69	1	1.0	II	F
JMA	−0.49	−1	3.0	II	F
LMD	−0.85	−1	3.0	II	P
GFDL	−0.78	−1	3.0	I	P
MPI	−0.51	−1	3.0	I	F
UIUC	−0.34	−1	3.0	II	F
COLA	−3.75	−2	4.0	II	F
MRI	−3.29	−2	4.0	I	P
CCC	−2.56	−2	4.0	I	F
NCEP1	−1.35	−2	4.0	II	F
NCEP2	−2.33	−2	4.0	I	–
NRL	−1.56	−2	4.0	II	P
IAP	−1.11	−2	4.0	II	P
SNG	−1.83	−2	4.0	II	P
ECMWF	−1.42	−2	4.0	II	P
BMRC	−2.58	−2	4.0	I	P
UGAMP	−1.14	−2	4.0	II	P
GISS	−2.10	−2	4.0	I	P
UKMO	−2.74	−2	4.0	I	P
YONU	−1.65	−2	4.0	II	F

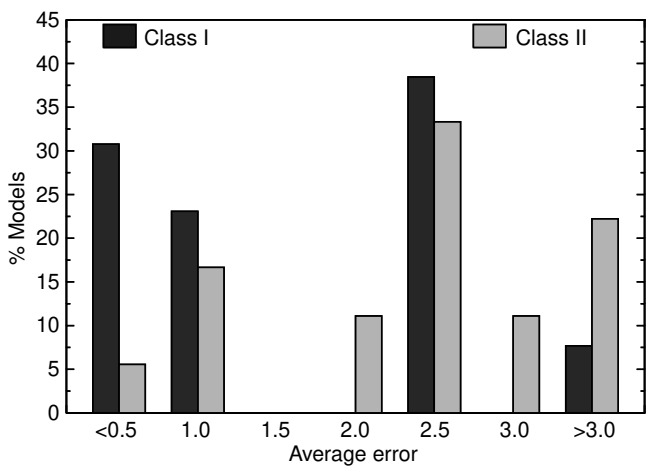

Fig. 14 Frequency distribution of the average error in simulation of anomalies of the events of 1982, 1987 and 1988 by models of classes I and II

a large range, varying from 0.01 to 0.67 for class I, and −0.39 to 0.60 for class II. All the 11 models with negative pattern correlation coefficients belong to class II (Table 3). Of these, 9 are associated with large errors (>2.3) in the simulation of the ENSO related seasons. The exceptions are ECMWF and UGAMP which simulate the interannual variation rather well, despite low pattern correlation coefficients. It is possible to attribute this to the success of these two models in simulating the teleconnection pattern and hence passing the SP test. However, there are three other models with negative pattern correlation coefficients which also pass the SP test (i.e. LMD, IAP and CSU) and which do not simulate the interannual variability well (errors>2.3). Hence, why ECMWF and UGAMP simulate interannual variation so well is not clear and needs to be investigated further. Further studies of the robustness of the skill of the models by analysis of multiple realisations as done for the ECMWF model (Sperber and Palmer 1996) may shed more light on this problem.

Of the 15 models with significant pattern correlation coefficients (≥ 0.3), 9 belong to class I and 6 belong to class II. In this subset, the fraction of models with good simulation of interannual variation in class I is 2/3 and in class II is 1/3. This suggests that achieving a realistic simulation of the seasonal migration of the rainbelt over the Asia-Pacific region will enhance the chance of simulating the interannual variation of the Indian monsoon associated with ENSO, when the mean pattern is reasonably well simulated. This hypothesis is supported by the one case in which two versions of the model, NCEP1 and NCEP2 belonging to classes II and I respectively. It is seen from Tables 3 and 6a that within the set of models with reasonable mean patterns (with pattern correlation coefficients ≥ 0.3), large errors occur for small as well as large pattern correlation coefficients (e.g., COLA and DNM). Thus, for models which simulate a realistic mean rainfall pattern over the Indian region (such as COLA, DNM, MGO), to improve the simulation of interannual variation of ENSO associated monsoon seasons, better simulation of seasonal migration of the rainbelt, over the Asia West Pacific region, is likely to be more effective than further improvement in simulation of the mean rainfall pattern over the Indian region.

5.3 Monsoon seasons without ENSO links

The observed and simulated precipitation anomalies for the seasons of 1979, 80, 86 are shown in Table 7. We note that, as expected, while in the case of the ENSO associated anomalies (Table 6a), five models captured all the three events here only one model captured all the events (with zero error). It is seen from Tables 6a, 7 that the GLA simulation has small errors for both the groups of seasons. We note that three of the top five

Table 7 Observed and simulated anomalies of all-India summer monsoon (June–September) rainfall (normalized with half the standard deviation), score for each event, average error, the class from Table 2 and the class based on SP test

Models	1979		1980		1986		$\sqrt{\{(\Sigma\varepsilon^2)/3\}}$	Classes	
	Anomaly	Score	Anomaly	Score	Anomaly	Score			SPtest
IMD (observations)	−2.25	2	1.31	2	−1.45	2			
RPN	−3.74	2	1.84	2	−2.20	2	0.0	I	F
GLA	−1.32	2	0.58	1	−1.35	2	0.58	I	P
SNG	−2.15	2	4.04	2	−0.72	1	0.58	II	P
NCAR	−1.73	2	0.62	1	−0.14	1	0.82	II	F
GFDL	−1.13	2	0.94	1	−0.53	1	0.82	I	P
CSU	−3.93	2	0.57	1	−0.23	1	0.82	II	P
SUNYA	−0.34	1	3.71	2	−0.66	1	0.82	II	F
COLA	−0.83	1	0.99	1	−0.68	1	1.00	II	F
DERF	−1.84	2	4.48	2	0.07	−1	1.73	II	F
DNM	−2.26	2	−0.28	−1	−4.31	2	1.73	II	F
UCLA	−1.07	2	−0.63	−1	−1.66	2	1.73	II	F
UIUC	0.98	−1	4.35	2	−2.88	2	1.73	II	F
MGO	−1.73	2	0.82	1	0.99	−1	1.83	II	P
MRI	0.11	−1	1.38	2	−0.58	1	1.83	I	P
CSIRO	0.11	−1	1.50	2	−0.43	1	1.83	I	P
LMD	0.14	−1	0.79	1	−1.76	2	1.83	II	P
CNRM	−1.40	2	−1.17	−2	−3.05	2	2.31	I	F
CCC	2.75	−2	1.59	2	−1.59	2	2.31	I	F
IAP	3.39	−2	1.08	2	−2.42	2	2.31	II	P
ECMWF	−1.20	2	3.03	2	1.22	−2	2.31	II	P
NCEP2	3.66	−2	0.33	1	−2.44	2	2.38	I	–
JMA	2.62	−2	3.02	2	−0.28	1	2.38	II	F
UGAMP	2.76	−2	2.64	2	−0.18	1	2.38	II	P
MPI	1.98	−2	1.27	2	−0.65	1	2.38	I	F
UKMO	1.32	−2	1.04	2	−0.05	1	2.38	I	P
GSFC	2.44	−2	0.93	1	−0.51	1	2.45	I	P
BMRC	3.13	−2	1.13	2	0.51	−1	2.89	I	P
NCEP1	2.58	−2	2.64	2	0.04	−1	2.89	II	F
GISS	0.13	−1	−2.59	−2	−0.14	1	2.94	I	P
NRL	3.23	−2	0.02	1	1.04	−2	3.32	II	P
YONU	2.66	−2	−0.56	−1	1.13	−2	3.70	II	F

models belong to class I and three of the bottom five belong to class II. As in the ENSO related seasons, on the whole, the models of class I perform better than those of class II, but the difference is much less. Thus, whereas the mean error for the ENSO associated anomalies for class I (1.34) is much smaller than that for class II (2.22); for this group of seasons the mean error for class I is 1.54 and that for class II is 1.88.

An unexpected result from this analysis is that a large number of models are able to simulate the sign of the anomaly in two years of this group i.e. 26 models for 1980 and 24 models for 1986. These are comparable to the number which simulated ENSO associated anomalies in 1987 and 88 i.e. 22 and 25 respectively. It turns out that the values of the error averaged over all the models for simulation of the seasons of the two groups are also very close. It is intriguing that for the monsoon seasons which are not associated with ENSO, on the whole, the simulations are as good as those for ENSO associated seasons. Further studies are required to understand this.

5.4 Variation during the AMIP decade

The overall skill of the models in simulating the interannual variation of the Indian summer monsoon during the AMIP decade (which comprised seven seasons with the amplitude of the anomalies larger than half the standard deviation) has been assessed by the root mean square error for each model computed by averaging the squared deviations of the normalized anomalies from the observed for each year (Table 8). For the decade as a whole also, the models with maximum (minimum) skill are those which pass (fail) the SP test. The proportion of class I (II) models is higher (lower) in the top (bottom) five models. As for the ENSO related seasons, the skill in simulating the interannual variation of the AMIP decade is larger for the classes of models that pass the SP test (2.27) and class I (2.39), than for those that failed the test (2.75) and class II (2.60). However, the difference in the class-average skills are much less when the decade as a whole is considered.

Table 8 Root mean square errors of simulated interannual variation of all-India summer monsoon rainfall during the AMIP decade for the different models

Models	Mean error
GLA	0.95
CSIRO	1.27
CSU	1.75
ECMWF	1.98
GSFC	2.03
SNG	2.13
CNRM	2.16
MRI	2.20
GFDL	2.30
UCLA	2.35
DNM	2.36
MGO	2.37
UIUC	2.44
NRL	2.49
UGAMP	2.52
JMA	2.58
RPN	2.61
DERF	2.76
MPI	2.79
BMRC	2.80
GISS	2.81
LMD	2.83
NCAR	2.85
SUNYA	2.87
UKMO	2.91
IAP	2.93
NCEP2	2.97
NCEP1	2.98
YONU	3.21
CCC	3.25
COLA	3.32

It is important to note that the ranking of models (as in Table 6a), is an intermediate step in identifying the general relationship between the skill of the model in simulating the interannual variation of the Indian Summer Monsoon and other features (such as whether they passed or failed the SP test or whether they belong to class I and II). This has revealed clearly the higher propensity of the models to simulate the variation if they pass the SP test or belong to class I. Unravelling of such general relationships is only possible with intercomparison of a large number of models as in AMIP. The hypotheses thus generated can be tested with further studies with some/all the models. The ranks of the models (rather of the specific versions studied) are not important as they will change with evolution of the models.

It must also be noted that the analysis presented involves only one run for each of the models for the observed SST during the AMIP decade. Clearly to assess the robustness of the response to the boundary conditions, multiple realisations are needed.

6 Summary and conclusions

The major results of the analysis of seasonal precipitation associated with the African, Indian and the Australian-Indonesian monsoon and the interannual variation of the Indian monsoon simulated by thirty atmospheric general circulation models during the AMIP decade are set out in the following paragraphs.

The seasonal migration of the major rainbelt observed over the African region, is reasonably well simulated by almost all the models. The Asia West Pacific region is more complex, because of the presence of warm oceans equatorward of heated continents. Whereas some models simulate the observed seasonal migration of the primary rainbelt, in several others this rainbelt remains over the equatorial oceans in all the seasons. Thus, the models fall into two distinct classes on the basis of the seasonal variation of the major rainbelt over the Asia West Pacific sector, the first (class I) comprising models with a realistic simulation of the seasonal migration and the major rainbelt over the continent in the boreal summer; and the second (class II) comprising models with a smaller amplitude of seasonal migration than observed. It turns out that such a classification is also useful for interpreting the simulation of the interannual variation of the Indian monsoon.

The mean rainfall pattern over the Indian region for July–August (the peak monsoon months) is even more complex because, in addition to the primary rainbelt over the Indian monsoon zone and the secondary one over the equatorial Indian ocean, another zone with significant rainfall occurs over the foothills of Himalayas just north of the monsoon zone. Eleven models simulate the mean rainfall pattern over the Indian region, reasonably realistically. About half of the models in this set belong to each of the two classes I, II. Thus a realistic simulation of this mean rainfall pattern seems to be equally likely for the two classes. However, whereas in models of class I of this category (e.g. GFDL) the rainfall over the Indian monsoon zone occurs in association with the seasonal migration of the planetary scale rainbelt, in models of class II of this category (e.g. COLA), the rainfall is associated with a regional system with a smaller longitudinal extent. In the simulations of ten models, the oceanic rainbelt and/or the orographic rainbelt dominate the primary rainbelt over the monsoon zone. In the intermediate category are models which simulate a primary rainbelt over the Indian region, but somewhat southward of the observed.

Very few models are able to capture all the fluctuations between good and poor monsoon seasons observed in the AMIP decade. We first consider the three summer monsoon seasons of 1982, 1987 and 1988 of contrasting rainfall anomalies which were associated with ENSO and the accompanying large variations of

the SST over the tropical Pacific. Even for these three seasons, only eleven models are able to simulate the monsoon anomaly of the correct sign. The majority of the models of this set which simulate realistically the anomalies of the three seasons, that is seven out of eleven, belong to class I. At the other end of the range, three models do not simulate the anomaly in any of the three seasons while in four others the sign of the anomaly of one season is simulated but the magnitude is small. Of these seven models, six belong to class II. On the whole, the skill in simulation of the excess/deficit events is much larger for models of class I than of class II. The mean rainfall pattern for the models of class I over the Indian region is closer to the observed than that for class II. This supports Sperber and Palmer's (1996) suggestion that a good rainfall climatology and proper simulation of the interannual variation are associated.

The study suggests that a realistic simulation of the seasonal variation over the Asia West Pacific sector will enhance the skill of simulating interannual variation of the Indian monsoon associated with ENSO. In the one case where we have two versions of the model i.e. NCEP1 and NCEP2, with NCEP1 in class II and NCEP2 in class I, the simulation of the interannual variation of the local response over the Central Pacific as well as the all-India monsoon rainfall are good for NCEP2 and poor for NCEP1, lending support to our hypothesis. Our results suggest that when the model climatology is reasonably close to the observed, to achieve a realistic simulation of the interannual variation of all-India monsoon rainfall associated with ENSO, the focus should be on improvement of the simulation of the seasonal variation over the Asia West Pacific sector, rather than further improvement of the simulation of the mean rainfall pattern over the Indian region.

Our analysis of the non-ENSO seasons with significant anomalies of monsoon rainfall has yielded some interesting results. As expected, the number of models which simulates a significant anomaly of the right sign is much smaller than for the seasons associated with ENSO. However, many models are able to simulate the anomaly of the correct sign for the seasons of 1980 and 1986.

It must also be noted that the analysis presented involves only one run for each of the models for the observed SST during the AMIP decade. Clearly to assess the robustness of the response to the boundary conditions, multiple realisations are needed.

Further studies are required on the sensitivity of the simulation of the mean seasonal rainfall pattern over the Indian region, as well as the seasonal variation over the Asia-Pacific sector to physics and numerics. The sensitivity of the nature of the local response to SST variations over the Pacific and the teleconnection with the Indian monsoon also needs to be studied. It appears that, in the 1990s the relationship between ENSO and the Indian monsoon may be different, since the warmth in the equatorial Pacific during 1992, 1993, 1994 was not associated with deficient monsoons. In the monsoon season of 1997, the all-India rainfall was slightly above normal in spite of the strong El Nino over the Pacific. The AMIP II runs may provide insight into the differing mechanisms at work between the decade studied here and the later years.

Acknowledgements This study could not have been carried out without the crucial input of the AMIP runs from the AMIP modelling groups. It is a pleasure to thank Prof. L. Gates, and the AMIP panel for making this study possible. Dr. Peter Gleckler and other members of PCMDI are thanked for all their efforts in giving us the model outputs as well as validation data in a convenient format. We are particularly indebted to Dr. Ken Sperber for constructive criticism and suggestions for improvement of an earlier version. We are very grateful to Susan Peterson for helping us and supplying information frequently over the last two years, and to Dr. Roger Newson for detailed suggestions which markedly improved the quality of the write up. We thank Dr. M. Manton and Dr. J. Shukla for critical comments. We would like to acknowledge particularly the interest shown by Dr. Eugenia Kalnay and Suranjana Saha of NCEP in this study and the time and effort of Dr. Suranjana Saha in making available results of an AMIP run of an improved version of the NCEP model. We benefited enormously from discussions with colleagues particularly Drs. J. Srinivasan, R. Narasimha and Ravi Nanjundiah of CAOS, IISc.

References

Arakawa A, Shubert WH (1974) Interaction of a cumulus ensemble with the large-scale environment, Part I. J Atmos Sci 31 : 674–704

Bjerknes J (1969) Atmospheric teleconnections from the equatorial Pacific. Mon Weather Rev 97 : 163–172

Charney JG (1969) The intertropical convergence zone and the Hadley circulation of the atmosphere. Proc WMO/IUGG Symposium on Numerical Weather Prediction, Japan Meteorological Agency

Chen L-X, Li W-L (1981) The heat sources and sinks in the monsoon region of Asia. Proc Symp on the summer monsoon in South East Asia, Hongzhou 1981, pp 86–101

Fennessy M, Shukla J (1994) Simulation and predictability of monsoons. Proc Int Conf Monsoon Variability and Prediction, Trieste May 9–13 1994 WMO/TD-619 : 567–575

Fennessy MJ, Kinter III JL, Kirtman B, Marx L, Nigam S, Schneider E, Shukla J, Straus D, Vernekar A, Xue, Y, Zhou J (1994) The simulated Indian monsoon: A GCM sensitivity study. J Clim 7 : 33–43

Gadgil S (1988) Recent advances in monsoon research with particular reference to Indian monsoon. Aust Meteorol Mag 36 : 193–204

Gadgil S, Guruprasad A, Sikka DR, Paul DK (1992) Intra-seasonal variation and simulation of the Indian summer monsoon. Simulation of inter-annual and intra-seasonal monsoon variability. Rep Workshop NCAR Boulder Colorado USA (October 1991) 21–24

Garcia O (1985) Atlas of highly reflective clouds for the global tropics: 1971–1983. US Department of Commerce, Env Res Lab Boulder Colo, USA

Gates WL (1992) AMIP: the Atmospheric Model Intercomparison Project. Bull Am Meteorol Soc 73 : 1962–1970

Grell GA (1993) Prognostic evaluation of assumptions used by cumulus parametrisations. Mon Weather Rev 121 : 764–787

Gruber A, Krueger AF (1984) The status of the NOAA outgoing longwave radiation data set. Bull Am Meteorol Soc 65 : 958–962

Hahn DG, Manabe S (1975) The role of mountains in the south Asian monsoon circulation. J Atmos Sci 32 : 1515–1541

Halley E (1686) An historical account of the trade winds and monsoons observable in the seas between and near the tropics, with an attempt to assign the physical cause of the winds. Philos Trans R Soc, London, pp 153–168
Hong S-Y, Pan H-L (1996) Nonlocal boundary layer vertical diffusion in a medium-range forecast model. Mon Weather Rev 124 : 2322–2339
Kalnay E, Kanamitsu M, Kistler R, Collins W, Deaven D, Gandin L, Iredell M, Saha S, White G, Woollen J, Zhu Y, Chelliah M, Ebisuzaki W, Higgins W, Janowiak J, Mo KC, Ropelewski C, Wang J, Leetmaa A, Reynolds R, Jenne R, Joseph D (1996) The NCEP/NCAR 40-year reanalysis project. Bull Am Meteorol Soc 77 (3) : 437–471
Kanamitsu M, Mo KC, Kalnay E (1990) Annual cycle integration of the NMC medium-range forecasting (MRF) model. Mon Weather Rev 118 : 2543–2567
Kuo HL (1965) On formation and intensification of tropical cyclones through latent heat release by cumulus convection. J Atmos Sci 22 : 40–63
Lau KM, Yang S (1996) The Asian monsoon and predictability of the tropical ocean-atmosphere system. Q J R Meteorol Soc 122 : 945–957
Laval K, Raghava R, Polchev J, Sadourny R, Forichon M (1996) Simulations of the 1987 and 1988 Indian monsoons using the LMD GCM. J Clim 9 : 3357–3371
Legates DS, Willmott CJ (1990) Mean seasonal and spatial variability in gauge-corrected, global precipitation. Int J Climatol 10 : 111–127
Manabe S, Hahn DG, Holloway J (1974) The seasonal variation of tropical circulation as simulated by a global model of atmosphere. J Atmos Sci 32 : 43–83.
Manabe S, Hahn G Jr, Holloway JL (1979) Climate simulation with GFDL spectral models of the atmosphere: effect of spectral truncation. Rept JOC Conf Climate Models WMO GARP Publ 22 (1) : 41–94
McBride JL (1987) The Australian summer monsoon. In: Chang CP, Krishnamurti TN (eds) Monsoon meteorology. Oxford University Press, pp 203–231
Miller MJ, Beljaars ACM, Palmer TN (1992) The sensitivity of the ECMWF model to the parametrisation of evaporation from the tropical oceans. J Clim 5 : 418–434
Miyakoda K, Sirutis J (1986) Manual of the E-physics. (Available from GFDL, Princeton University PO Box 308 Princeton, NJ 08542)
Palmer TN, Brankovic C, Viterbo P, Miller MJ (1992) Modeling interannual variations of summer monsoons. J Clim 5 : 399–417
Pan H-L, Mahrt L (1987) Interaction between soil hydrology and boundary layer developments. Boundary Layer Meteorol 38 : 185–202
Pan H-L, Wu W-S (1995) Implementing a mass flux convection parametrisation package for the NMC medium range forecast model. NMC Office Note 409 40 pp
Parthasarathy B (1984) Some aspects of large-scale fluctuations in the summer monsoon rainfall over India during 1871–1978. PhD Thesis, University of Pune, India, September 1984
Parthasarathy B, Rupa Kumar K, Munot AA (1992) Forecast of rainy-season food grain production based on monsoon rainfall. India J Agri Sci 62(1) : 1–8
Parthasarathy B, Munot AA, Kothawale DR (1994) All-India monthly and seasonal rainfall series; 1871–1993. Theor Appl Climatol 49 : 217–224
Phillips TJ (1994) A summary documentation of the AMIP model. PCMDI Rep 18 Program for Climate Model Diagnosis and Intercomparison 343 pp
Ramage CS (1971) Monsoon meteorology. Academic Press 296 pp
Rao YP (1976) Southwest monsoon India Meteorological Department. Meteorological Monograph Synoptic Meteorology 1/1976, Delhi, 367 pp
Rasmusson EM, Carpenter TH (1983) The relation between eastern equatorial Pacific sea surface temperatures and rainfall over India and Sri Lanka. Mon Weather Rev 111 : 517–528
Riehl H (1954) (ed) Tropical meteorology. McGraw Hill, New York
Riehl H (1979) (ed) Climate and weather in the tropics. Academic Press, New York
Ropelewski CF, Halpert MS (1987) Global and regional scale precipitation patterns associated with the high index phase of the southern oscillation. Mon Weather Rev 115 : 1606–1626
Ropelewski CF, Halpert MS (1996) Quantifying southern oscillation-precipitation relationships. J Clim 9 : 1043–1059
Schemm JK, Schubert S, Terry J, Bloom S (1992) Estimates of monthly mean soil moisture for 1979–1988. NASA Tech Memo 104571 GSFC Greenbelt 260 pp
Sela J (1980) Spectral modeling at the National Meteorological Center. Mon Weather Rev 108 : 1279–1292
Sikka DR (1980) Some aspects of the large-scale fluctuations of summer monsoon rainfall over India in relation to fluctuations in the planetary and regional scale circulation parameters. Proc Indian Acad Sci (Earth Planet Sci) 89 : 179–195
Sikka DR, Gadgil S (1980) On the maximum cloud zone and the ITCZ over India longitude during the southwest monsoon. Mon Weather Rev 108 : 1840–1853
Slingo JM (1987) The development and verification of a cloud prediction scheme for the ECMWF model. Q J R Meteorol Soc 113 : 899–927
Slingo JM, Blackburn M, Thuburn J, Steenman-Clark L, Brugge R, Hoskins B (1992) Synoptic validation of climate models: aspects of variability in the tropics of the UGAMP general circulation model. Proc Seminars on Model Validation, Reading, England ECMWF pp 265–279
Slingo JM, Blackburn M, Betts A, Brugge R, Hoskins B, Miller M, Steenman-Clark L, Thuburn J (1994) Mean climate and transience in the tropics of the UGAMP GCM: sensitivity to convective parameterisation. Q J R Meteorol Soc 120 : 881–922
Spencer RW (1993) Global oceanic precipitation from the MSU during 1979–91 and comparisons to other climatologies. J Clim 6 : 1301–1326
Sperber KR, Palmer TN (1996) Interannual tropical rainfall variability in general circulation model simulations associated with the Atmospheric Model Intercomparison Project. J Clim 9 (11) : 2727–2750
Sperber K, Hameed S, Potter GL, Boyle JS (1994) Simulation of the northern summer monsoon in the ECMWF model: sensitivity to horizontal resolution. Mon Weather Rev 122 : 2461–2481
Srinivasan J, Smith GL (1996) Meridional migration of tropical convergence zones. J Appl Meteorol. 35 : 1189–1202
Sud YC, Walker GK (1992) A review of recent research on improvement of physical parametrisations in the GLA GCM. In: Sikka DR, Singh SS (eds) Physical processes in atmospheric models, Wiley Eastern, pp 424–479
Tao S, Chen L (1987) A review of recent research on the East Asian summer monsoon in China. In: Monsoon meteorology. Chang CP, Krishnamurti TN (eds) Oxford University Press, pp 60–92.
Tiedtke M (1983) The sensitivity of the time-mean large scale flow to cumulus convection in the ECMWF model. Proc ECMWF Workshop on Convection in Large-scale Models, 28 Nov-1 Dec 1983 ECMWF Reading England 297–316
TOGA monsoon climate research (1990) Report of the second session of the monsoon numerical experimentation group. WMO